Anthropocene 55 (2026) 100563

Contents lists available at ScienceDirect

Anthropocene

journal homepage: www.elsevier.com/locate/ancene

Centennial-scale climate variability and human land-use shaped vegetation and lake dynamics in southern Spain over the past three millennia

Gonzalo Jiménez-Moreno[a,*], Erik J. de Boer[a], Jon Camuera[b], Antonio García-Alix[a,b], Fernando Gázquez[c,d], Aurora Castillo-Baquera[a], Lucía Martegani[c,d], Miguel Rodríguez-Rodríguez[e], Marta Rodrigo-Gámiz[a], Francisco J. Jiménez-Espejo[b], Lu Chenao[f], José S. Carrión[g]

[a] Departamento de Estratigrafía y Paleontología, Universidad de Granada, Spain
[b] Instituto Andaluz de Ciencias de la Tierra (IACT), CSIC-UGR, Armilla, Spain
[c] Department of Biology and Geology. University of Almería, Almería, Spain
[d] Andalusian Centre for Global Change – Hermelindo Castro University of Almería, Spain
[e] Physical, Chemical and Natural Systems, Pablo de Olavide University, Seville, Spain
[f] Department of Geosciences and Geography, Faculty of Science, University of Helsinki, Finland
[g] Department of Plant Biology (Botany Area), Faculty of Biology, University or Murcia, Murcia, Spain

A R T I C L E I N F O

Dataset link: Pollen data Laguna Grande de Archidona

Keywords:
Vegetation
Temperature
Precipitation
Lake dynamics
Climate
Human impact
Late Holocene
Western Mediterranean

A B S T R A C T

Mediterranean vegetation has been profoundly shaped by the interaction of climate variability and human activities, and understanding the timing, magnitude, and drivers of these transformations is essential for predicting ecosystem responses in an especially climate-sensitive region. In this study we present a high-resolution palynological record spanning the last ~3150 years from Laguna Grande de Archidona (LGA), a lake in southern Spain, to reconstruct vegetation history, fire activity, identify major Late Holocene climatic and lake-environment phases, and disentangle the relative roles of climate variability and human activity in controlling landscape evolution. Quantitative temperatures were estimated by a calibration derived from the Eurasian Modern Pollen Database v2 (EMPDv2) using the Weighted Averaging-Partial Least Squares (WA-PLS) calibrated regression method. Temperature primarily controlled elevational shifts of vegetation belts, while variations in effective moisture (precipitation minus evaporation) governed lake level fluctuations in the study area. Temperatures were highest coinciding with a period of higher humidity during the Iberian Roman Humid Period (IRHP). Subsequently, cooling is observed during the Early Middle Ages (EMA) and the Little Ice Age (LIA). The alternation of persistent North Atlantic Oscillation (NAO) modes probably played an important role in controlling the humid-arid cycles observed at LGA. Anthropogenic impact in the area becomes particularly clear during the last millennium, when intensified olive cultivation progressively transformed the landscape.

1. Introduction

Reconstructing past environmental dynamics is essential for understanding the complex interactions between climate variability and human activities (PAGES2k Consortium, 2017; MedECC, 2020). In the Mediterranean region, where long-term human occupation has profoundly altered natural ecosystems, disentangling climatic and anthropogenic signals in paleoecological records remains a major challenge (Gil-Romera et al., 2009; Carrión et al., 2007; 2010; Alba-Sánchez et al., 2021). Pollen analysis provides a powerful tool to trace past vegetation changes and infer climatic trends, offering insights into how landscapes have responded to both natural forcing and cultural transformations through time (Carrión et al., 2010; Ramos-Román et al., 2016; 2018; Mesa-Fernández et al., 2018).

Southern Spain occupies a critical biogeographical position at the interface between the temperate and arid climatic domains of the western Mediterranean (Lionello et al., 2006). Following the Early and Middle Holocene humid and thermal maximum, a long-term trend toward cooler and more arid conditions developed, significantly affecting vegetation patterns (Jiménez-Moreno et al., 2022). This region has also

* Corresponding author.
E-mail address: gonzaloj@ugr.es (G. Jiménez-Moreno).

https://doi.org/10.1016/j.ancene.2026.100563
Received 24 May 2026; Received in revised form 22 June 2026; Accepted 23 June 2026
Available online 25 June 2026
2213-3054/© 2026 The Author(s). Published by Elsevier Ltd. This is an open access article under the CC BY license (http://creativecommons.org/licenses/by/4.0/).

experienced marked climatic oscillations during the Late Holocene, superimposed upon millennia of intensive land use and settlement (Anderson et al., 2011; Jiménez-Moreno et al., 2013; Ramos-Román et al., 2018). Increasing evidence indicates that human disturbance played a crucial and spatially heterogeneous role, particularly from the Middle to Late Holocene onward (Carrión et al., 2010). Activities such as burning, pastoralism, and ploughing associated with agrarian and metallurgical societies became increasingly influential, especially during the Chalcolithic and Bronze Age periods, when vegetation changes closely correlate with human impact in numerous pollen records from southern Iberia, such as Acebrón (Stevenson and Harrison, 1992), Las Madres (Stevenson, 1985), Medina (Reed et al., 2001), Baza (Carrión et al., 2007), Gádor (Carrión et al., 2003), Baeza and Úbeda (Fuentes et al., 2007). The interplay between natural and anthropogenic factors has controlled the composition and structure of Mediterranean vegetation, from evergreen oak woodlands and pine forests to open shrublands and agricultural landscapes (Carrión et al., 2010; Anderson et al., 2011; Jiménez-Moreno and Anderson, 2012; Ramos-Román et al., 2018). Identifying the timing, magnitude, and drivers of these shifts is necessary to understanding current ecological changes in a region especially vulnerable to climate warming and desertification (IPCC, 2022).

Laguna Grande de Archidona (LGA; Málaga Province, southern Spain) offers a unique sedimentary archive for investigating these dynamics (Jiménez-Moreno et al., 2025a). Located within an endorheic karstic basin, and being a permanent lake, the site provides excellent conditions for the continuous preservation of pollen and other previously studied paleoenvironmental sedimentary proxies (Jiménez-Moreno et al., 2025a; Gázquez et al., 2025). Its location at relatively low elevation, between the thermo- and mesomediterranean vegetation belts, as well as in the present-day intensively cultivated interior of Andalusia makes it particularly suitable for evaluating the regional vegetation response to both climatic fluctuations and the progressive expansion of human land use since the late Bronze Age.

This study presents a high-resolution palynological record from LGA covering the past ~3150 years. The main objectives are to (1) reconstruct the vegetation history of the basin and its surroundings, (2) identify the major climatic phases and lake environment changes during the Late Holocene, and (3) distinguish the relative influence of climatic versus anthropogenic drivers on landscape evolution. By integrating palynological, sedimentological and historical evidence, this study provides a refined perspective on long-term climate–human–environment interactions in the western Mediterranean.

2. Study site

LGA (37º06’28.30’’N, 4º18’14.88’’W; 794 m a.s.l.) is part of the Archidona Lakes Nature Reserve, a protected wetland system located near the towns of Salinas and Archidona in the province of Málaga, southern Spain (Fig. 1). The reserve lies within an endorheic basin and comprises two brackish to saline lakes, LGA to the north and Laguna Chica (LCA) to the south, which together support a rich diversity of bird species. The reserve covers approximately 0.06 km^2, surrounded by a 1.87 km^2 buffer zone, yielding a total protected area of 1.93 km^2. LGA occupies an average flooded surface of 0.06 km^2 and drains a relatively

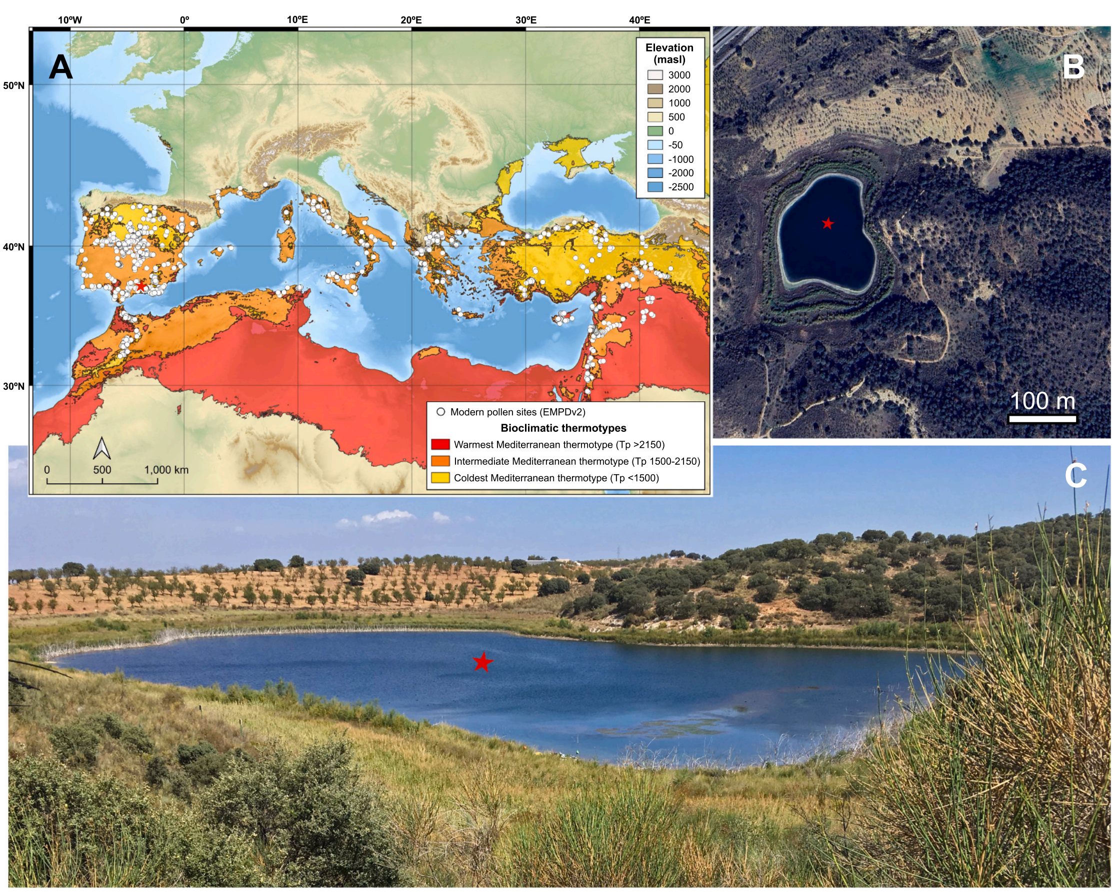

Fig. 1. Location of the study site Laguna Grande de Archidona (LGA). (A) Map of the Mediterranean area showing the modern pollen sites (white dots) used for the pollen-based quantitative temperature reconstruction of Laguna Grande de Archidona. The calibration-set is based on 1797 Mediterranean modern pollen sites, based on the EMPDv2 (Davis et al., 2020). Red, orange and yellow areas represent the warmest, intermediate and coldest Mediterranean thermotypes used to select the Mediterranean pollen calibration-set.The location of LGA in southern Spain is indicated by a red star. (B) Aerial photo of LGA (from Google Earth) and coring location (red star). (C) Photograph of LGA and sediment core location (red star). Note the almond and olive crops in the background.

small watershed of 0.14 km^2. With a maximum depth of 13.4 m, LGA is among the deepest natural permanent lake systems in southern Spain.

The LGA area features a continental Mediterranean climate (mean annual temperature: 14.8 °C; summer: 23.1 °C; winter: 7.7 °C). Southern Spanish precipitation is strongly modulated by the North Atlantic Oscillation (NAO) (Hurrell et al., 2013). Positive NAO phases divert storms northward, causing droughts, while negative phases shift storm tracks southward, bringing more Atlantic moisture and rainfall, especially in winter. Rainfall mainly occurs from October to May, peaking in December associated with humid Atlantic westerlies, alongside springtime convective storms. Between 2017 and 2023, mean annual precipitation was 418 mm, markedly lower than the 574 mm average recorded in the late 20th century (WorldClim v2.1 climate data for 1970–2000; Fick and Hijmans, 2017).

Natural tree vegetation in the LGA area at 794 m a.s.l. is characterized by the predominance of mesomediterranean vegetation belt (between 700 and 1300 m; Rivas-Martínez, 1987) with evergreen oaks (*Quercus rotundifolia*), wild olive trees (*Olea europaea* var. *sylvestris*) and fewer deciduous oaks (*Q. faginea*). *Crataegus*, *Retama*, *Rosa*, *Ulex*, *Genista* and *Phlomis* are the characteristic shrubs in the area. Herbs are dominated by several species of Poaceae, Asteraceae, Lamiaceae and Amaranthaceae. In Granada and Málaga, the lower elevation thermomediterranean bioclimatic belt (approximately 0–700 m, locally somewhat higher on sunny slopes) is characterized by a very warm climate, marked summer drought, and sclerophyllous, thermophilous vegetation. Typical tree species include *Olea europaea* var. *sylvestris*, *Ceratonia siliqua*, *Quercus coccifera*, *Chamaerops humilis* (mostly in coastal areas), *Pinus halepensis* and *Tetraclinis articulata*. Among shrubs, *Pistacia lentiscus* and *P. terebinthus*, *Rhamnus alaternus*, *R. lycioides*, *Myrtus communis* and *Retama monosperma* are abundant. Common grasses (Poaceae) include *Macrochloa tenacissima*, *Brachypodium retusum*, *Lygeum spartum* and *Aegilops* spp.

Anthropogenic activities in the study region are mostly characterized by *Prunus dulcis* (almond) and *Olea* (olive) crops and cereal and sunflower seed cultivation. LGA is immediately surrounded by a dense *Juncus,* Cyperaceae and *Tamarix* belt that makes difficult the access to the lake shore. LGA is also colonized by different communities of aquatic submerged macrophytes including *Potamogeton*, *Myriophyllum* and *Chara*.

3. Materials and methods

3.1. Sediment core recovery

The 276 cm-long LGA sedimentary record is a composite sequence derived from two adjacent cores: the short core LGA−19–03 and the

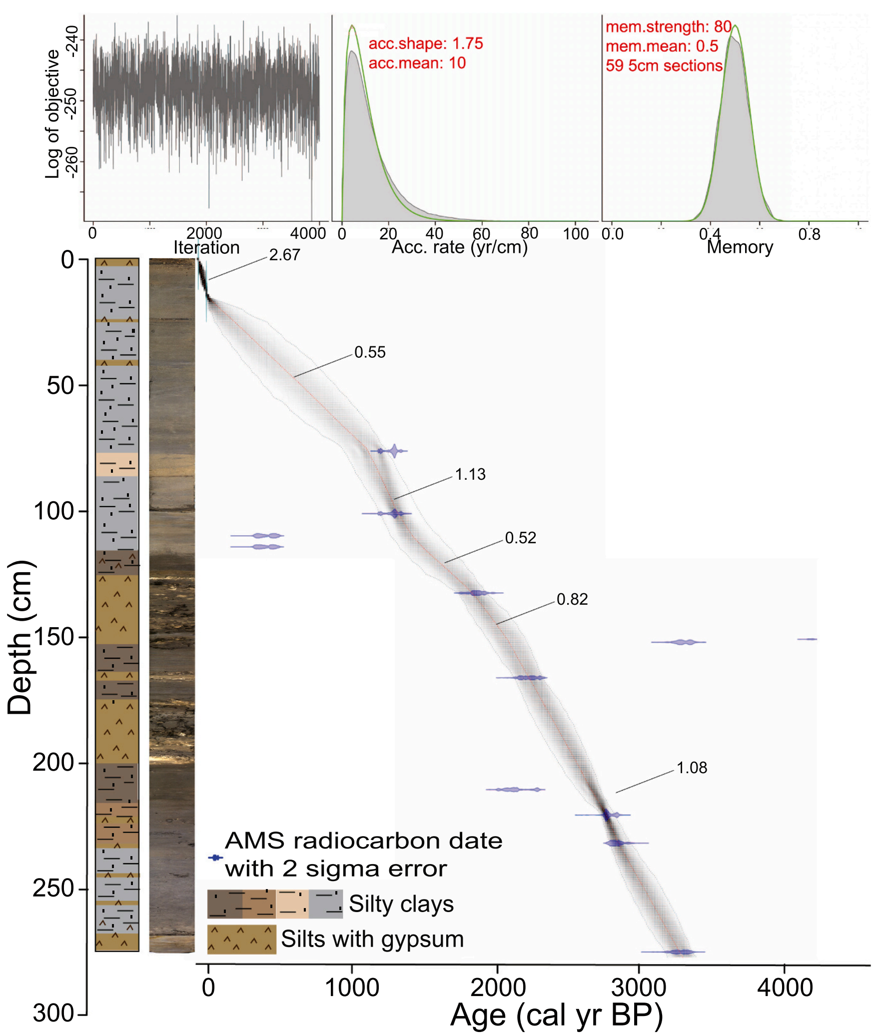

Fig. 2. LGA sedimentary record and Bayesian age model (95% confidence interval and red median line) with estimated sedimentary rates in mm/yr. The calibrated ^{14}C dates and their associated uncertainties are depicted in blue. The accumulation rate plot illustrates both the prior and posterior distribution of accumulation rates, with green and grey lines respectively. Similarly, the memory plot displays the prior and posterior distribution of model memory, again delineated by green and grey lines. The log-posterior time-series demonstrates a consistent and stable model performance. Modified from Jiménez-Moreno et al. (2025a).

long core LGA−19–04. These cores were retrieved from the depocenter of the LGA basin in September 2019 using a floating platform anchored to the lake bottom. Sampling was performed with a universal corer fitted with a plexiglass tube (Aquatic Research, Inc.) for the short core and a Livingstone square-rod piston corer for the long core (Fig. 2). The lake depth at the coring site was 8.9 m.

3.2. Core description and chronological control

The cores were transported to the University of Granada (UGR), stored in a refrigerated room at 4ºC and were eventually split and imaged in the laboratory at UGR and Centro de Instrumentación Científica (CIC, UGR), respectively. The lithology and magnetic susceptibility (MS) were previously described in Jiménez-Moreno et al., (2025a). The age model was previously constructed by Jiménez-Moreno et al. (2025a) using a total of 12 AMS radiocarbon dates and a $^{239+240}$Pu activity profile obtained in the topmost 20 cm of the LGA−19–04 core (Table 1; see Jiménez-Moreno et al., 2025a).

3.3. Palynological analysis

The LGA sedimentary record, containing the past ~3300 cal yr BP based on the age model described in Jiménez-Moreno et al., (2025a) (Fig. 2), was sampled for palynological analysis every ~4 cm. A total of 64 samples of two cubic centimeters were collected. The pollen extraction method followed a modified Fægri and Iversen (1989) method. One tablet with a known number of *Lycopodium* spores for calculation of pollen concentration was added to the samples. Sediment samples were processed with HCl (35%) and HF (45%) to remove the carbonates and silicates, respectively, from the sediment, and concentrate the organic matter. The samples were sieved at 10 µm to remove particles smaller than the pollen grains. The residual material, together with glycerin, was mounted on microscope slides. Counting, and identification, of palynomorphs was carried out with a Leica DM1000 LED transmitted light microscope at 400x magnification. Pollen atlases, such as Beug (1961) and pollen reference material of plants that occur in southern Spain were used for certain identifications. Pollen percentages in each analyzed sample have been calculated with respect to the total sum of terrestrial pollen, excluding aquatic macrophytes including Cyperaceae, *Sparganium-Typha*, *Myriophyllum* and *Potamogeton*. The most representative pollen types with occurrences higher than 1% are shown in Fig. 3. The percentages of non-pollen palynomorphs (NPPs), including algae such as *Botryococcus, Spirogyra* and *Zygnema*, oocytes of the aquatic flatworm *Neorhabdocoela,* thecamoebians, spores of *Sporormiella* dung fungus and mycorrhizal chlamydospores of *Glomus* have been calculated with respect to the total sum of terrestrial pollen plus NPPs and are shown in Fig. 4. Cluster analyses of the pollen and NPPs data were performed using the program CONISS (Grimm, 1987), with the aim of grouping samples with similar pollen assemblages into pollen zones (Figs. 3 and 4). Charcoal particles bigger than 30 microns were counted in the palynological slides. Charcoal concentration (charcoal particles/cm^3) was calculated using the *Lycopodium* tracer concentration (Fig. 4) in this way: #charcoal particles/#*Lycopodium* tracers *13,761 (being 13,761 the number of *Lycopodium* tracers in 1 tablet).

Table 1
Age data for the LGA sedimentary sequence. Radiometric ages were calibrated using IntCal20.14c curve (Reimer et al., 2020) with Calib 8.2 (http://calib.org/calib/). Radiocarbon dates were analyzed at BETA Analytic laboratory (https://www.radiocarbon.com/). Plutonium analyses were carried out at Northern Arizona University, USA by Michael E. Ketterer.

ID	Depth (cm)	Material dated	Conventional age (^{14}C yr BP)	Median age cal BP	IRMS δ^{13}C (‰)
Surface	0			−69	
Pu	12.6–13.1			−13	
576890	75.95–76.45	organic sediment	1360 ± 30	1289	−30.3
563346	100.6–101.6	plant material	1370 ± 40	1293	−26.9
560857	109.55–110.05	plant material	360 ± 30	414	−28.4
544700	114.2	plant material	350 ± 30	396	−27.7
576891	132.35–132.85	organic sediment	1940 ± 30	1864	−28.4
563347	150.5–151.5	plant material	3890 ± 30	4333	−36.9
563348	151.7–152.7	plant material	3090 ± 30	3295	−30.6
576892	165.7–166.7	organic sediment	2210 ± 30	2230	−25.7
544701	210.1–211.1	plant material	2140 ± 30	2128	−20.4
544702	220.7	plant material	2660 ± 30	2769	−16.2
576893	231.4–232.4	organic sediment	2740 ± 30	2823	−27.2
576889	274.6–275.6	organic sediment	3060 ± 30	3277	−26.5

Modified from Jiménez-Moreno et al. (2025a).

3.4. Temperature estimations

Mean annual temperatures were quantitatively reconstructed using fossil pollen data from LGA and a regionally restricted calibration set of 1797 modern pollen sites from the Mediterranean bioclimatic region of the Eurasian Modern Pollen Database v2 (EMPDv2) (Davis et al., 2020; Figs. 1 and 5). Following the bioclimatic classification of López-Fernández and López-Fernández (2018), this calibration dataset encompasses three Mediterranean thermotypes based on positive annual accumulated temperature (Tp, expressed in tenths of degrees Celsius): warmest Mediterranean thermotype (Tp >2150), the intermediate thermotype (Tp 1500–2150) and the coldest thermotype (Tp <1500) (Fig. 1). Because LGA is located within the intermediate Mediterranean thermotype, including all three types broadens the temperature range variations detectable in the reconstruction.

Taxonomic harmonization between fossil and modern assemblages yielded 333 taxa, standardized using Plants of the World Online database and the Integrated Taxonomic Information System. To minimize non-climatic local noise, aquatic plants and taxa indicative of halophytic environments or strong local ecological signals, such as Amaranthaceae, Asteroideae and Cichorioideae, were excluded. Cultivated or reforested taxa (*Olea*, Myrtaceae/*Eucalyptus*) were also omitted. Some other taxa that may be affected by reforestation and human impact, such as *Pinus*, *Castanea* and *Juglans*, could have affected the reconstructed temperature values. However, although these taxa can affect the abundance of vegetation in modern pollen samples and their effect cannot be entirely ignored, their impact on the reconstruction is low due to their low abundance in the Laguna Grande de Archidona record.

Modern temperature values were obtained from the WorldClim v2.1 database (Fick and Hijmans, 2017). Quantitative temperature reconstruction was done using the Weighted Averaging-Partial Least Squares (WA-PLS) calibrated regression method, which assumes a unimodal relationship between taxon abundances and climatic variables, and is robust to spatial autocorrelation (Telford and Birks, 2005). To reduce noise in the calibration set, we applied a square root transformation to the species data and the reliability of the reconstruction was evaluated through leave-one-out cross validation. The two component WA-PLS model was selected because additional components tend to increase the risk of overfitting and reduce predictive performance. All the analyses were conducted using the C2 software (version 1.8.0) (Juggins, 2022). The statistical performance of the reconstructed mean annual temperature provided a coefficient of determination (R^2) of 0.51 and a root mean square error of prediction of 2.17 ºC. Although pollen-based climate reconstructions provide robust regional records, they can be

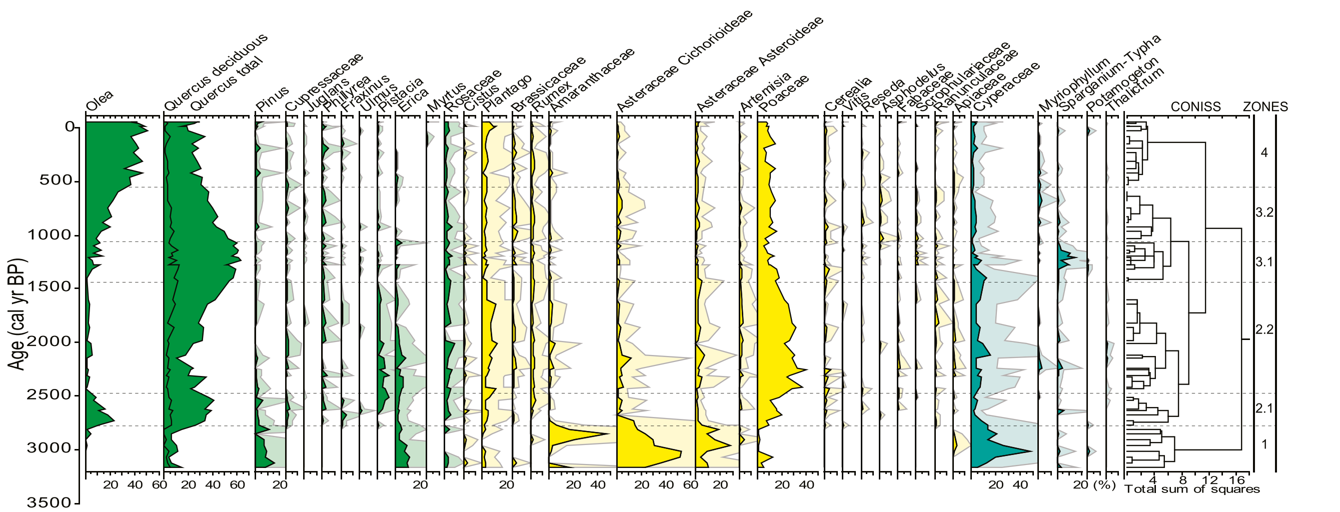

Fig. 3. Detailed pollen diagram from the LGA sedimentary record showing percentages of selected taxa (higher than 1%). In green, yellow and blue are the trees, herbs and wetland angiosperm taxa, respectively. The pollen zonation on the right was made using cluster analysis provided by CONISS (Grimm, 1987). Light shadings indicate a 5 × exaggeration scale.

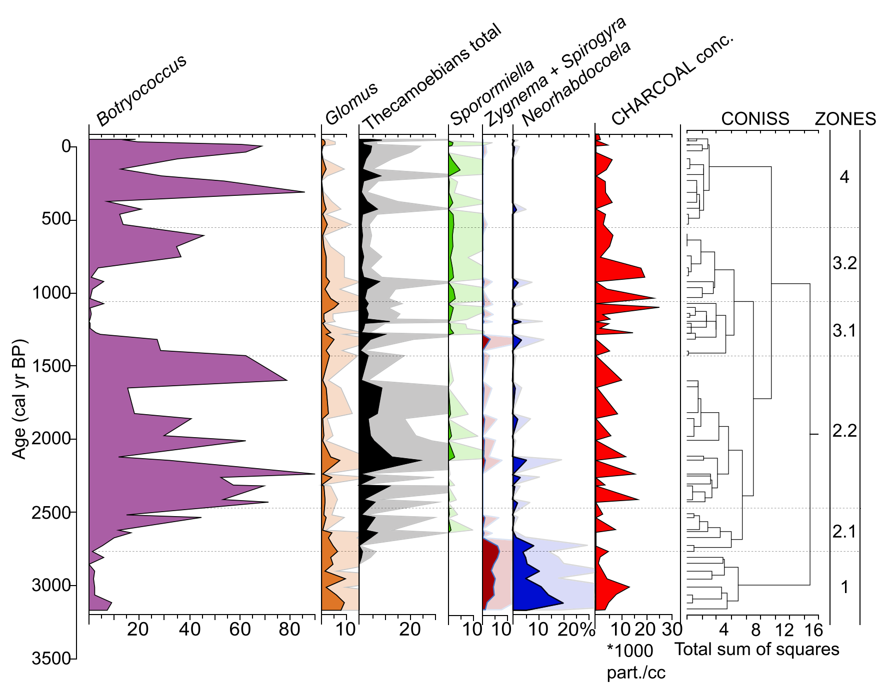

Fig. 4. Detailed non-pollen palynomorph (NPPs) and charcoal diagram from the LGA core. The NPPs zonation on the right was made using cluster analysis provided by CONISS (Grimm, 1987). Light shadings indicate a 5 × exaggeration scale.

limited by taphonomic biases such as differential grain preservation and the selective degradation of fragile taxa, potentially introducing a systematic artifact into quantitative paleoclimate models. The estimation of precipitation was initially explored using the same methodology. However, the results were strongly influenced by temperature covariance and were therefore not considered sufficiently robust for quantitative interpretation.

3.5. *Mineral and geochemical analyses*

X-ray diffraction (XRD) analysis of sediment samples was also previously done, facilitating the identification of the principal mineral phases (Jiménez-Moreno et al., 2025a). High-resolution elemental records were generated using X-Ray fluorescence (XRF) core scanner analyses on the sedimentary cores (Jiménez-Moreno et al., 2025a). A principal component analysis (PCA) on these XRF data was carried out using the Past 4.05 program (Hammer et al., 2001). The variability of the XRF data are mostly explained by the PC1 (with a 58% of the variance), with a siliciclastic group (PC1 +) made up of Si, K, Ti, Fe, Rb and Zr covarying together and showing an opposite pattern of change than gypsum-carbonate components such as S, Ca, Sr and Mn (PC1-) (see Jiménez-Moreno et al., 2025a; Figs. 6 and 7).

In a previous study, Gázquez et al. (2025) measured triple oxygen ($\delta^{17}O$, $\delta^{18}O$ and $^{17}O_{excess}$) and hydrogen ($\delta^{2}H$ and D-excess) isotopes in the LGA lacustrine gypsum from the studied sedimentary record to quantify changes in summer atmospheric relative humidity between 2600 and 1450 cal yr BP (650 BCE – 500 CE) (Fig. 6).

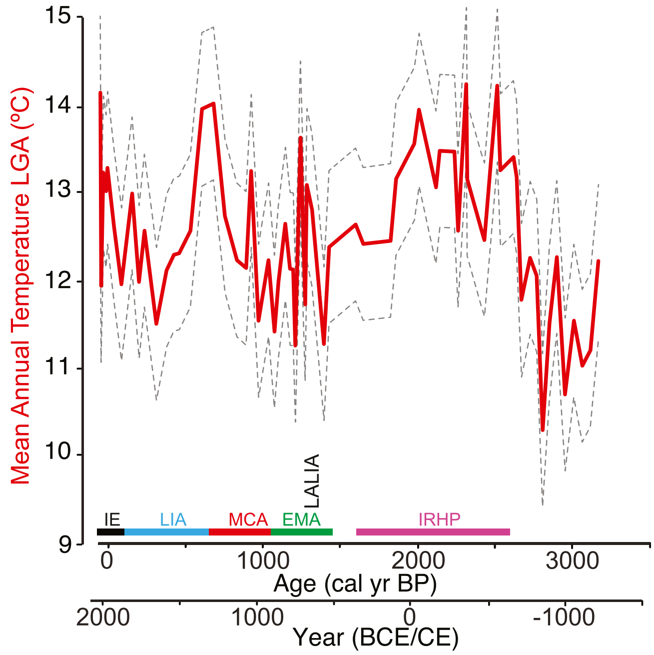

Fig. 5. Pollen-inferred mean annual temperature from the LGA record and associated standard error of prediction (eSEP; dashed black thin lines) for each sample. The duration of historic periods such as the Iberian Roman Humid Period (IRHP), Late Antique Little Ice Age (LALIA), Early Middle Ages (EMA), Medieval Climate Anomaly (MCA), Little Ice Age (LIA) and Industrial Era (IE) is indicated.

4. Results

The LGA pollen record is made up of 64 samples covering the past ~3150 years. The samples were generally characterized by low pollen concentration but provided sufficient pollen (average number of 210 pollen grains per sample) for statistical analyses (Sánchez Goñi et al., 2002; Djamali and Cilleros, 2020). Samples from the interval between 3300 and 3150 cal yr BP were barren in pollen. The pollen record is generally characterized by varying abundances of forest taxa with respect to the herbaceous component (Fig. 3). Abundant NPPs include various algae, *Glomus* and other spores, thecamoebians and eggs of aquatic flatworms (Fig. 4). Charcoal concentration varies throughout the record (Figs. 4 and 7). The pollen and NPPs frequencies fluctuate considerably through time and can be subdivided into several environmental and climatically distinct periods (zones) that roughly agree with a climatic subdivision previously done based on the geochemistry and sedimentology by Jiménez-Moreno et al. (2025a) (Figs. 6 and 7). Below, we describe the LGA pollen and NPPs results for each of the identified zones.

4.1. Pollen and NPPs zone 1 between ~3150 and 2700 cal yr BP (~264 – 211 cm)

This palynological zone is characterized by the highest abundance of herbs in the LGA record, mostly represented by Asteraceae Cichorioideae (reaching up to 50% at ~3000 cal yr), Asteraceae Asteroideae (averaging 15%), Amaranthaceae with a peak of 50% at ~2850 cal yr and *Artemisia* with a maximum of 4.5% at ~2900 cal yr BP (Fig. 3). With respect to forest taxa, *Pinus* shows the highest abundances of the record in this zone, with a peak of ~15% at ~3100 cal yr BP. Ericaceae also shows highest abundances of the record during this time. The helophyte Cyperaceae shows maximum occurrences of 50% at 3000 cal yr BP (Fig. 3). With respect to the NPPs, this zone is characterized by the highest abundances of *Glomus* and Zygnemataceae (*Zygnema*+*Spirogyra)* of the record. Low *Botryococcus* and absence of *Sporormiella* and thecamoebians also characterize this zone. The charcoal concentration displays a peak (up to 12500 charcoal fragments/cm^3) at ~3000 cal yr BP.

4.2. Pollen and NPPs zone 2 between ~2700 and 1400 cal yr BP (~211 – 110 cm)

4.2.1. Pollen and NPPs subzone 2.1 between ~2700 and 2500 cal yr BP (~211 – 195 cm)

A peak in *Olea* (20%), evergreen and deciduous *Quercus* (40%), *Pistacia* (10%), *Phillyrea*, *Fraxinus* and Cupressaceae occurred in this subzone. Significant changes in the herbs occurred, with the decrease in Asteraceae Cichorioideae, Asteraceae Asteroideae and Amaranthaceae. In contrast, *Plantago*, *Rumex* and Poaceae increased during this period (Fig. 3). With respect to the NPPs, an increase in *Botryococcus* and in thecamoebians, and first occurrences of *Sporormiella,* occurred. A decrease in *Zygnema* and *Spirogyra* is observed. The charcoal concentration is relatively low (below 7000 charcoal fragments/cm^3) during this subzone (Fig. 4).

4.2.2. Pollen and NPPs subzone 2.2 between ~2500 and 1400 cal yr BP (~195 – 110 cm)

This subzone is characterized by the decrease in *Olea* and *Pinus.* Evergreen and deciduous *Quercus* show a decrease first, reaching a minimum ~2150 cal yr BP of 10%, and then an increase until the end of this subzone. *Pistacia* and Ericaceae show high abundances. With respect to the herbs, maximum abundances of Poaceae, reaching up to 40%, and *Artemisia* (with 4% at ~1800), occurred. *Plantago* is also abundant. The NPPs are characterized by maximum abundances of *Botryococcus* with a maximum of 90% at ~2250 cal yr BP. Low *Glomus* and absence of *Zygnema* and *Spirogyra* also characterize this subzone. *Botryococcus* decreased between ~2200 and 1600 cal yr BP while thecamoebians show maxima and *Glomus* and *Sporormiella* increased. *Botryococcus* algae show another peak between ~1600 and 1400 cal yr BP whereas *Sporormiella* and thecamoebians decreased. The charcoal concentration increased with respect to the previous subzone to values of ~15000 charcoal fragments/cm^3.

4.3. Pollen and NPPs zone 3 between 1400 and 600 cal yr BP (~110 – 47 cm)

The highest abundance of evergreen and deciduous *Quercus* occurred in this zone. An increasing trend in *Olea* is observed. Poaceae decreased to average values around 15%. This pollen zone can be further subdivided into two subzones: NPPs subzone 3.1 between 1400 – 1100 cal yr BP and NPPs subzone 3.2. between 1100 and 600 cal yr BP.

4.3.1. Pollen and NPPs subzone 3.1 between 1400 and 1100 cal yr BP (~110 – 76 cm)

Highest abundances of evergreen and deciduous *Quercus*, reaching up to 62%, occurred. A peak in Cyperaceae and *Sparganium-Typha* of 15% is observed at ~1200 cal yr BP. With respect to the NPPs, *Botryococcus* decreased considerably reaching minimum values at the end of the subzone while *Sporormiella* increased. Two *Glomus* peaks at ~1300 and ~1100 cal yr BP characterize this subzone. The charcoal concentration increased reaching a maximum of ~23800 charcoal fragments/cm^3 at ~1100 cal yr BP.

4.3.2. Pollen and NPPs subzone 3.2 between 1100 and 600 cal yr BP (~76 – 47 cm)

Evergreen and deciduous *Quercus* are abundant but decreased progressively from 60% to 30%, whereas *Olea* shows an increasing trend from 10% to 35%. *Botryococcus* increased at the end of this subzone, showing a peak at ~750–600 cal yr BP. *Sporormiella* is abundant throughout the subzone. *Glomus* and thecamoebians decreased in this subzone. Two peaks in charcoal concentration are observed at ~1000

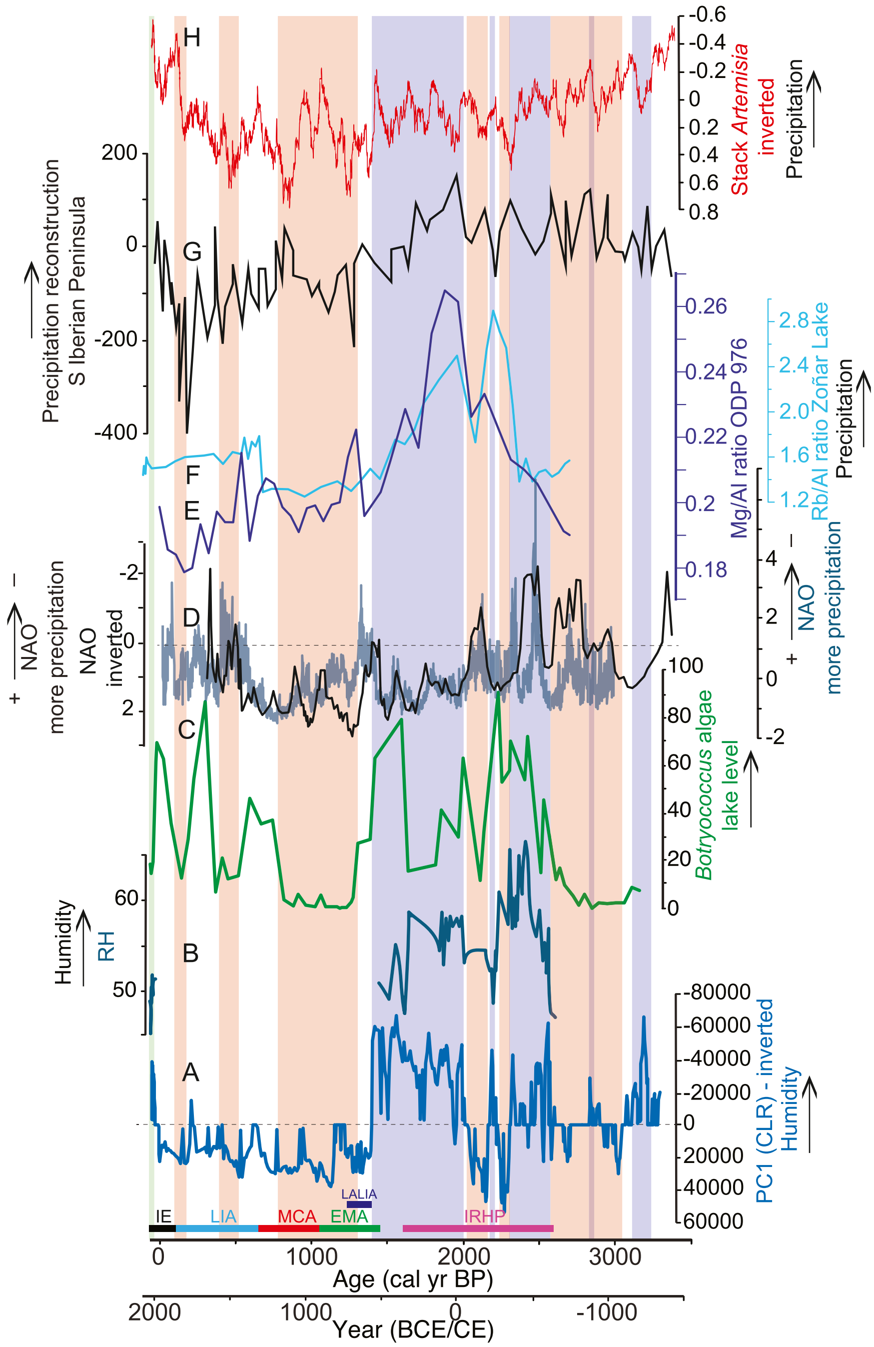

Fig. 6. Comparison of the multiproxy record from LGA (A-C) with other regional and hemispheric records of humidity and paleoprecipitation (D-H). (A) PC1 of LGA XRF (note that it is inverted; Jiménez-Moreno et al., 2025a). (B) Relative Humidity (RH) estimated by gypsum geochemistry at LGA (Gázquez et al., 2025). (C) Abundance of *Botryococcus* algae in the LGA sediment core indicating lake level. (D) Inverted NAO reconstruction (Olsen et al., 2012) in black and NAO reconstruction based on speleothem growth from Baker et al. (2015) in blue. (E) Mg/Al ratio from site ODP 976, Alboran Sea (Martín-Puertas et al., 2010). (F) Rb/Al ratio from Zoñar Lake, Córdoba (Martín-Puertas et al., 2010). (G) Precipitation reconstruction from S Iberian Peninsula based on pollen records (Ilvonen et al., 2022). (H) Stack of *Artemisia* xerophyte from Iberia and Morocco (inverted) (Camuera et al., 2023). In light blue and pink color shadings are the identified humid and arid periods, respectively. In light green shading is the human impact period. The duration of historic periods such as the Iberian Roman Humid Period (IRHP), Late Antique Little Ice Age (LALIA), Early Middle Ages (EMA), Medieval Climate Anomaly (MCA), Little Ice Age (LIA) and Industrial Era (IE) is indicated.

and ~900–850 cal yr BP.

4.4. Pollen and NPPs zone 4 between 600 cal yr BP and Present (~47 – 0 cm)

Olea is the most abundant genus and shows an increasing trend, reaching up to 50% in the 20th century (between 37 and −15 cal yr BP). Evergreen and deciduous *Quercus* shows an overall decreasing trend but depicts a peak of 33% at 84 cal yr BP (1866 CE) and another peak of 30% at present. *Plantago* increased in this subzone with a maximum abundance of 12% at −6 cal yr BP (1956 CE). *Botryococcus* shows variability with three minima (ca. 10%) at around 500, 150 and −48 cal yr BP and two maxima (80–70%) at 300 and 0 cal yr BP. Thecamoebians show peaks during the *Botryococcus* minima. *Sporormiella* varies but shows continuous occurrences in this zone. The charcoal concentration decreased in this subzone until present-day.

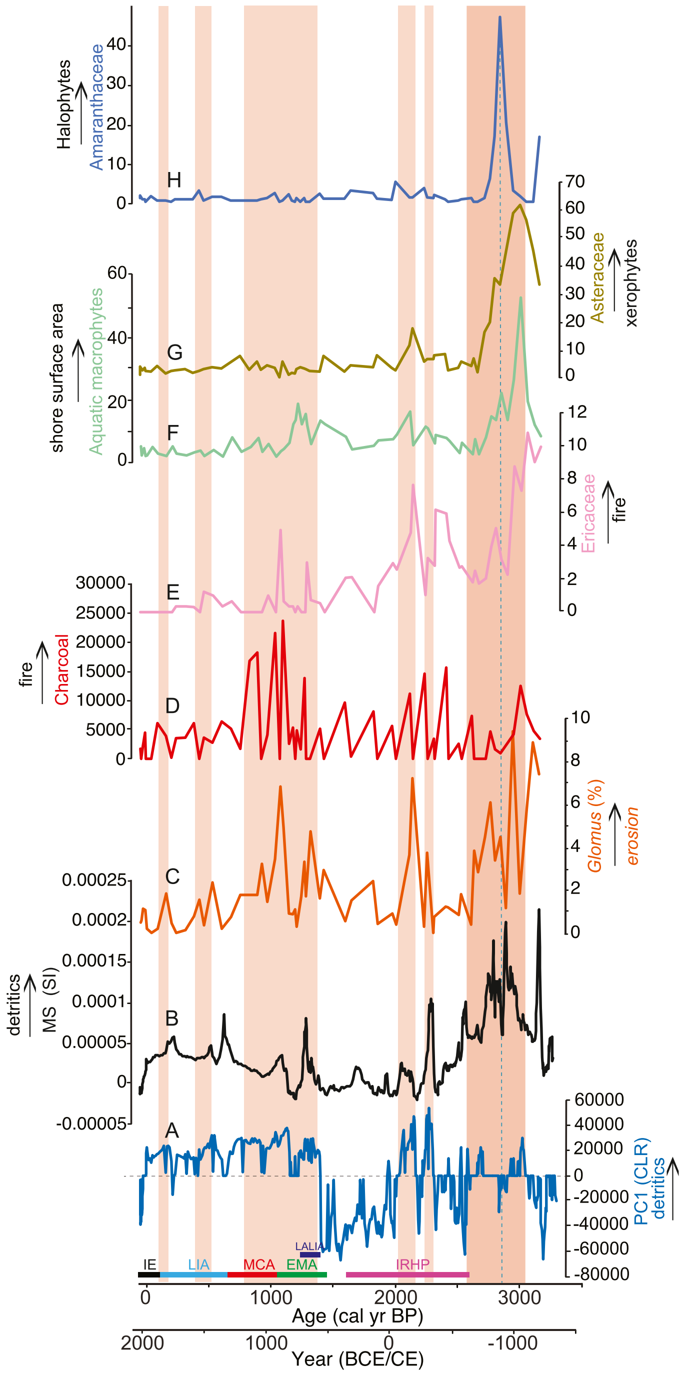

Fig. 7. Comparison of the multiproxy records from LGA of aridity, low lake level, erosion and fire. (A) PC1 of LGA XRF (Jiménez-Moreno et al., 2025a). (B) MS (in SI units) from LGA (Jiménez-Moreno et al., 2025a). (C) Abundance of *Glomus* (%). (D) Charcoal concentration. (E) Ericaceae abundance (%). (F) Abundance of aquatic macrophytes including Cyperaceae, *Sparganium-Typha* and *Myriophyllum*. (G) Xerophyte Asteraceae abundance (%). (H) Halophyte Amaranthaceae abundance (%). In light pink color shadings are the identified arid periods. The duration of historic periods such as the Iberian Roman Humid Period (IRHP), Late Antique Little Ice Age (LALIA), Early Middle Ages (EMA), Medieval Climate Anomaly (MCA), Little Ice Age (LIA) and Industrial Era (IE) is indicated.

4.5. Pollen-inferred quantitative mean annual temperatures

The pollen-based mean annual temperature reconstruction for the past ~3150 cal yrs BP shows values oscillating between 10.3 ºC and 14.2 ºC (Figs. 5 and 9). The record begins with low values with minima below 11 ºC at ~3050, 2950, 2800 and 2670 cal yr BP. Temperatures increased after that and several peaks above 13.5–14 ºC are recorded between ~2600 and 1800 yr BP, including a maximum value of 14.2 ºC at ~2500 cal yr BP. Temperatures decreased after 1800 stabilizing around 12.5 ºC until ~1400 cal yr BP. A further decrease in temperature values occurred then and four minima around 11.5 ºC are recorded at ~1394, 1250, 1200 and 1070 cal yr BP. Temperatures increased afterwards, and two peaks above 13 ºC are recorded at 920 and 680–600 cal yr BP (1030 and 1270–1350 CE), interrupted by a minimum around 12.2 ºC between 890 and 750 cal yr BP (1060–1200 CE). Subsequently, a decrease in temperatures is observed with minimum temperatures, reaching 11.5 ºC between ~520 (1430 CE) and 310 cal yr BP (1640 CE). Temperatures increased above 13 ºC between 150 and −6 cal yr BP (between 1800 and 1956 CE). A decrease down to 12 ºC is recorded at −48 cal yr BP (1998 CE) and temperatures raised rapidly up to 14.1 ºC, between then and −53 cal yr BP (2003 CE; Fig. 9).

5. Discussion

5.1. Pollen and NPPs proxy interpretation

Palynological analysis from lake sediments from southern Spain has previously been reported as a proxy for regional vegetation change related to climate variability and anthropogenic activity (Anderson et al., 2011; Jiménez-Moreno and Anderson, 2012; Ramos-Román et al., 2016, 2018; Mesa-Fernández et al., 2018; Camuera et al., 2019). For example, increases in forest species such as *Quercus*, *Olea* and *Pistacia* in the pollen records from this arid area, point to increases in humidity (Camuera et al., 2019). This is because trees need relatively high soil water supply, while herb taxa can thrive under more dry conditions and are abundant during arid periods (Camuera et al., 2019). Fluctuations in their frequencies during the latest Pleistocene and Holocene sediments might then reflect climate shifts (see for example Anderson et al., 2011; Jiménez-Moreno and Anderson, 2012). In addition, forest species responded to changes in climate with vertical displacements upwards when climate warmed, and downwards when climate cooled. The movements in elevation of the vegetation assemblages during the Pleistocene and Holocene due to millennial-scale climatic variations can be recognized by changing pollen abundances (Camuera et al., 2019). LGA is situated at the boundary between the thermomediterranean (0–700 m a.s.l.) and mesomediterranean (700–1400 m a.s.l.) vegetation belts and changes in temperature are going to be evidenced in the area by abundance variations between more thermophilous and xerophilous taxa such as Poaceae (including *Macrochloa*, for example), *Artemisia* and *Pistacia*, typical from the low-elevation thermomediterranean vegetation belt and *Quercus*, the most abundant species in the higher-elevation mesomediterranean vegetation (Rivas-Martínez, 1989). Synthetic pollen relationships or ratios can be used as proxies for changes in vegetation and climate oscillations (Carrara et al.,1984; Toney and Anderson, 2006). In this case, the thermomediterranean/mesomediterranean (T/M) pollen ratio points to the relative changes in elevation between the two altitudinal bioclimatic assemblages mostly driven by changes in temperature. In this way, the increases in thermomediterranean species that occur today at lower elevations than LGA can be explained as an upward shift of these taxa induced by warming (Figs. 8 and 9).

The increase in pollen grains from cultivars such as *Olea*, Cerealia, *Vitis* and other weeds indicating disturbed environments created by agriculture such as *Plantago* or *Rumex* could indicate anthropogenic activities such as agriculture and land use (Carrión et al., 2010).

Lake levels from southern Spain also responded to past climate changes, predominantly conditioned by variations in the precipitation-evaporation balance, with higher lake levels during cold and/or humid periods and lower lake levels during warm and/or arid periods, which also controlled the lake ecosystem (Anderson et al., 2011; Camuera et al., 2018, 2019; López-Avilés et al., 2022). Planktonic

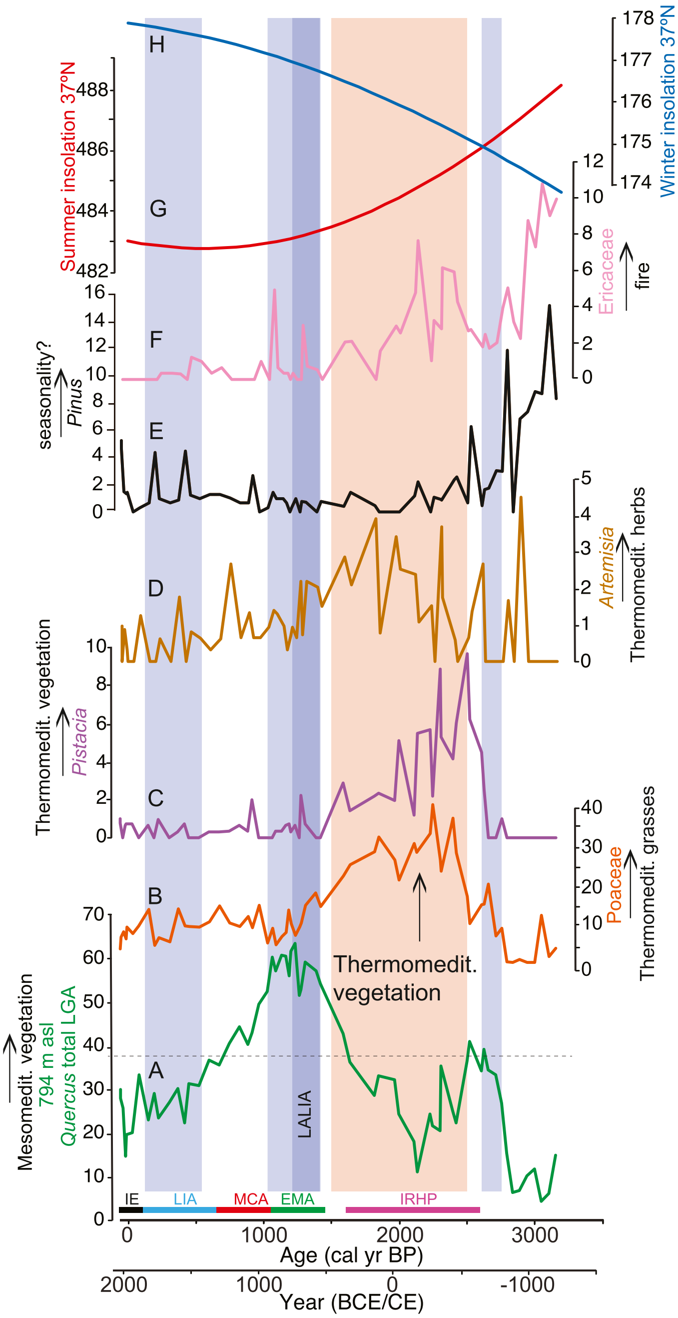

Fig. 8. Comparison of the main pollen taxa from LGA indicating thermomediterranean and mesomediterranean vegetation belts and their dynamics controlled by temperature oscillations, with *Pinus* forest, indicating high seasonality, and Ericaceae, indicating fire, with summer and winter insolation. (A) Abundance of *Quercus* total representing the mesomediterranean vegetation in the study area. (B) Poaceae abundance representing the thermomediterranean vegetation. (C) *Pistacia* abundance representing the thermomediterranean vegetation. (D) *Artemisia* abundance representing the thermomediterranean vegetation. (E) *Pinus* abundance (seasonality). (F) Ericaceae abundance (fire). (G) Summer insolation for 37ºN (Laskar et al., 2004). (H) Winter insolation for 37ºN (Laskar et al., 2004). In light blue and pink color shadings are the identified cold and warm periods, respectively. The duration of historic periods such as the Iberian Roman Humid Period (IRHP), Late Antique Little Ice Age (LALIA), Early Middle Ages (EMA), Medieval Climate Anomaly (MCA), Little Ice Age (LIA) and Industrial Era (IE) is indicated.

microalgae (*Botryococcus*, *Spirogyra*, *Zygnema*), wetland macrophytes (Cyperaceae, *Sparganium-Typha*), and other organisms (such as the aquatic flatworm *Neorhabdocoela*), are conditioned by lake levels and shore surface area. *Botryoccocus*, a colonial green microalga, has previously been interpreted as a eutrophic lake water indicator (Guy-Ohlson, 1992; Jiménez-Moreno et al., 2007) but also an indicator of pelagic conditions (Carrión, 2002). While *Botryococcus* abundance is interpreted here primarily as a lake-level indicator, this is because its close similarity to previous lake level and precipitation-humidity estimations from LGA (Jiménez-Moreno et al., 2025a; Gázquez et al., 2025; Fig. 6). However, its response may also be influenced by changes in trophic state and productivity, and therefore should be considered a multi-factor proxy. Water shallowing and shore colonization by marginal emergent water aquatic macrophytes are indicated by increases in Cyperaceae and *Typha* (Carrión, 2002). *Neorhabdocoela* has been described as a proxy for shallow and eutrophic lake conditions. This is inferred because *Neorhabdocoela* is restricted to the phytal zone (feeding for example on rotifers and diatoms) and produces oocytes, thick-walled resting-eggs, for propagation and for surviving unfavorable ecological conditions during drought (Haas, 1996).

High abundances of *Glomus* endomycorrhizal fungus in sediment samples from paleoecological records have been related to increased rates of soil erosion and other mechanical soil disturbances (Anderson et al., 1984; Van Geel et al., 1989). *Sporormiella* is a coprophilous fungal spore, and in other Holocene lake sedimentary records, its presence has been used as a key proxy of large herbivore abundance, especially livestock and thus human impact (Baker et al., 2013). Thecamoebians are freshwater amoeboid protozoans, characterized by an agglutinated test held together by organic cement, that occur in a variety of wetland habitats including moss, soil, peat and standing water from tropical to polar environments (Boudreau et al., 2005). Their abundance has been reported as an indicator of eutrophic environments (Escobar et al., 2008; Jiménez-Moreno and Anderson et al., 2012).

In addition, sediment charcoal concentration from lake records is a proxy for fire activity (Whitlock and Anderson, 2003). This is because charred particles accumulate in sediments during and following a nearby fire event. Therefore, stratigraphic levels with abundant charcoal are inferred to be evidence of past fires and the abundance of charcoal particles can be taken as an indication of regional fire occurrence (Whitlock and Anderson, 2003).

The relative abundance of the above-mentioned pollen and NPPs changed through the different climatically distinct periods (zones), providing us with information about lake depth, nutrients and productivity, climate and human activity through time. Here we compare the pollen-inferred paleoclimate quantitative data with the palynological data and other paleoclimatic records from the study region and we show that the surrounding vegetation and organisms inhabiting the LGA environment responded very sensitively to climate changes that occurred in the last ∼3000 years in the western Mediterranean area. Although both the T/M ratio and the quantitative temperature reconstruction are derived from the same pollen dataset, they represent independent analytical approaches (relative assemblage shifts versus transfer-function modelling), which strengthens confidence in the inferred climatic signal.

5.2. Pre-Roman period between ∼3150 and 2600 cal yr BP (1200 – 650 BCE)

Overall, arid climate conditions are interpreted for this period around LGA. This is indicated by low lake levels (low *Botryococcus*; Fig. 6) and high emergent aquatic macrophytes (Cyperaceae) and halophytes (Amaranthaceae; Fig. 6) indicating a larger emerged wet-saline surface area, high abundance of Asteraceae (xerophytes) and indicators of high erosion (*Glomus*, MS; Fig. 6). *Glomus*, MS and XRF PC1 covary together throughout the record, meaning more erosion during arid periods. The highest abundances of Zygnemataceae (*Zygnema*+*Spirogyra)*

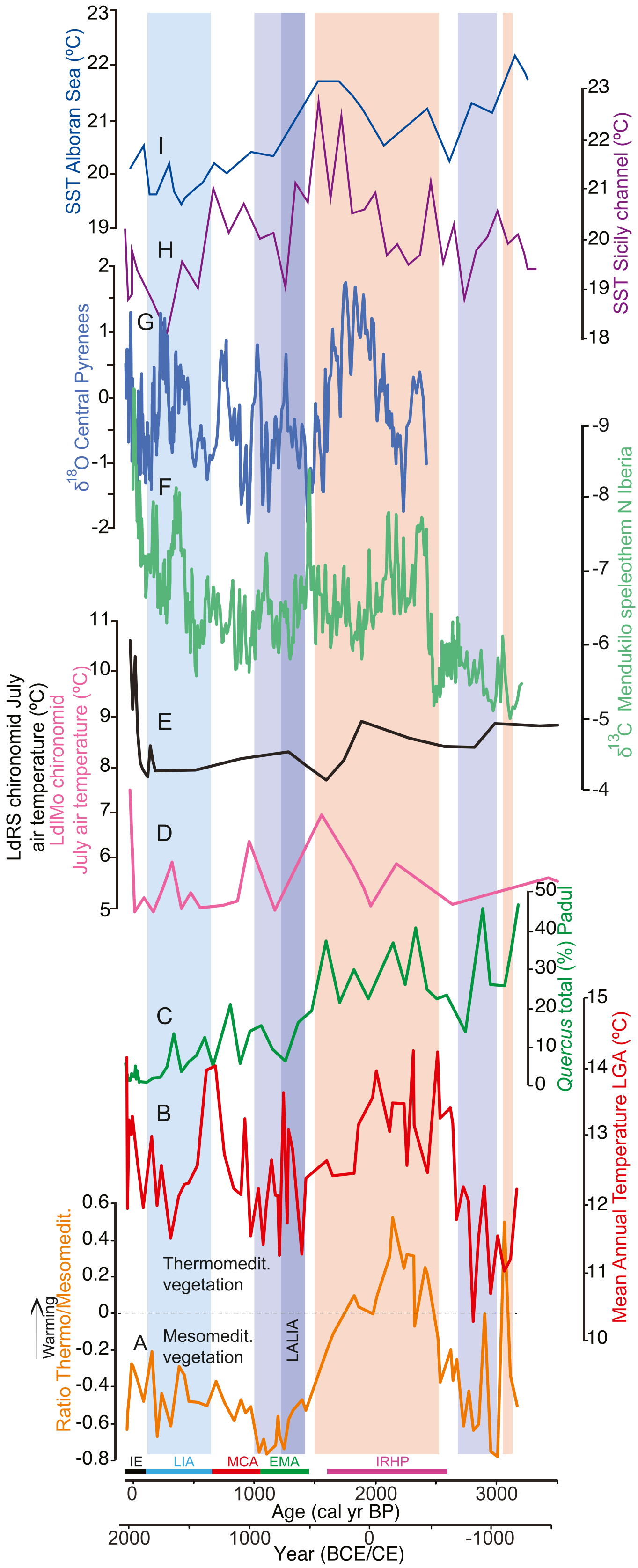

(caption on next column)

Fig. 9. Comparison of the thermomediterranean/mesomediterranean (T/M) temperature proxy and pollen-based estimation from LGA with other regional records of temperature. (A) Thermomediterranean/mesomediterranean (T/M) ratio from LGA. (B) Pollen-based mean annual temperature estimation from LGA in º Celsius. (C) Total abundance (%) of *Quercus* from Padul−15–05 (Ramos-Román et al., 2018). (D) Chironomid-inferred July air temperature from LdlMo (Jiménez-Moreno et al., 2025b). (E) Chironomid-inferred July air temperature from LdRS (Jiménez-Moreno et al., 2023b). (F) Temperature-related $\delta^{13}C$ record from Mendukilo speleothem (Bernal-Wormull et al., 2023). (G) Temperature-related $\delta^{18}O$ record from central Pyrenees speleothems (Bartolomé et al., 2024). (H) Sea surface temperature (SST) estimation from Sicily Channel (Margaritelli et al., 2020). (I) Sea surface temperature (SST) estimation from Alborán Sea (Rodrigo-Gámiz et al., 2014). In light blue and pink color shadings are the identified cold and warm periods, respectively. The duration of historic periods such as the Iberian Roman Humid Period (IRHP), Late Antique Little Ice Age (LALIA), Early Middle Ages (EMA), Medieval Climate Anomaly (MCA), Little Ice Age (LIA) and Industrial Era (IE) is indicated.

and *Neorhabdocoela* in the record (Fig. 4) suggests meso- to eutrophic stagnant shallow water under a mild climate (Carrión, 2002; Jiménez-Moreno et al., 2023a).

The relatively high *Pinus* percentages between 3150 and 2800 cal yr BP (Fig. 8) may reflect increased aridity and enhanced summer drought tolerance. Our taxonomic identifications are at the genus level but two species of *Pinus* could potentially grow at the elevation of the LGA area at present: *P. halepensis* and *P. pinaster* (Rivas-Martínez, 1987), and both could have contributed pollen to the sedimentary record. In Mediterranean lowlands, rising aridity in the Late Holocene contributed to declines in mesic forest elements and increases in pines, because these species are adapted to marked summer drought (Pérez-Sanz et al., 2013) and high summer-winter insolation contrast (Laskar et al., 2004). The progressive decreasing trend in *Pinus* throughout the LGA sequence could have been due to the progressive cooling and decrease in seasonal contrast that occurred in the Middle and Late Holocene due to the decrease and increase in summer and winter insolation, respectively (Fig. 8). However, besides these changes in seasonality, ecological competition likely also played a role.

The pollen record indicates that climate between ~3150 and 3000 cal yr BP, besides being arid, could have also been warm. This is indicated by a peak in thermomediterranean taxa and thus in the thermomediterranean/mesomediterranean (T/M) pollen ratio (Fig. 9). Warm and overall arid conditions could have triggered gypsum precipitation in the LGA between 3200 and 3100 cal yr BP (Jiménez-Moreno et al., 2025a; see XRF PC1 in Fig. 6). Ericaceae also show maximum abundances at this time. The Ericaceae family is adapted to fire and increase their occurrence after fires because they vigorously resprout from stumps or lignotubers (for example in *Erica arborea*), their germination is stimulated after fire (heat, ash) and they show rapid recolonization of burned soils (Keeley et al., 2012). An arid and warm climate could have triggered more fire events in the area, favoring the spread of Ericaceae around LGA. A peak in charcoal concentration at 3000 cal yr BP indicates fire occurrence in the area at that time (Figs. 4 and 7), which could support this hypothesis. However, an anthropogenic origin of this fire activity cannot be ruled out, as other records from southern Spain indicate increased charcoal deposition and human activity in the region. Notably, high levels of atmospheric lead pollution and charcoal were recorded at the same time, which have been linked to intense metallurgical activity (Anderson et al., 2011; García-Alix et al., 2013).

Cooler conditions occurred between 3000 and 2600 cal yr BP (Fig. 9). This is supported by the increase in mesomediterranean taxa such as *Quercus* (pollen subzone 2.1; Figs. 3 and 9), and thus a decrease in the T/M ratio, and pollen-based temperature minima at ~2950, 2800 and 2670 cal yr BP. A peak in *Olea* is also observed between 2800 and 2600 cal yr BP, perhaps indicating cultivation of olive trees or enhanced humid conditions. Regional cooler conditions most-likely occurred in the study area at this time, as a coeval cooling event around 2700–2600 cal yr BP has been observed in the sea surface temperature records from the western Mediterranean associated with the Homeric grand solar minimum (ca. 800 BCE; Margaritelli et al., 2020; Fig. 9).

The highest peak of Amaranthaceae occurred at 2850 cal yr BP, during a short humid period previously identified by geochemical ratios during an overall arid phase (see XRF PC1 in Figs. 6 and 7). This could have been due to enhanced salinity in the lake shore area favoring the growth of halophytes such as Amaranthaceae due to a brief rise of groundwater levels (Jiménez-Moreno et al., 2025a).

From an archaeological point of view, this overall arid period coincides in southern Spain with a transitional period of fragmentation and cultural reconfiguration during the Late Bronze Age, with defensive settlements and changes in production and funerary practices (Mederos Martín, 2021).

5.3. The warm and humid IRHP (2600–1400 cal yr BP; 650 BCE – 550 CE)

The period between 2600 and 1400 cal yr BP (including pollen subzone 2.2) is interpreted in this study by the occurrence of highest humidity in the LGA area. This period roughly coincides with the IRHP defined by Martín-Puertas et al. (2009) between 2600 and 1600 cal yr BP. The highest abundances of *Botryococcus* point to highest LGA lake levels at that time (Fig. 6). This agrees with the previous interpretation of this interval as the wettest of the LGA record based in the geochemistry (XRF PC1; Jiménez-Moreno et al., 2025a) and the isotopic analysis of the gypsum hydration water (Gázquez et al., 2025; Fig. 6), which suggest that atmospheric relative humidity was ~10% higher than at present-day during the wetter phase of the IRHP at ~2400 cal yr BP. Regional indications of high humidity at this time come from Zoñar Lake, where also *Botryoccocus* is highest, also interpreted as high-lake levels due to high precipitation and freshwater input in the lake (Martín-Puertas et al., 2009). Contemporaneous high humidity has also been recorded in the nearby Sierra Nevada (Jiménez-Moreno et al., 2013; Ramos-Román et al., 2016; 2018). The prevailing humid conditions in the Mediterranean region during the IRHP, especially between 2500 and 2400 cal yr BP, have been attributed to elevated winter rainfall, likely originated by persistent negative NAO conditions, as suggested by Olsen et al. (2012) and Baker et al. (2015) (Jiménez-Moreno et al., 2025a; Gázquez et al., 2025; Fig. 6).

Centennial-scale variations in humidity occurred during the IRHP indicated by oscillations in the *Botryococcus* abundance and confirmed by the MS and geochemistry (Jiménez-Moreno et al., 2025a) and the RH estimated by the gypsum geochemistry (Gázquez et al., 2025) (Fig. 6). Notably, an arid phase occurred centered at ~2100 cal yr BP indicated by many proxies at LGA (Fig. 6). This is confirmed by a peak of high aquatic macrophytes, halophytes (Amaranthaceae), Asteraceae and *Glomus* indicating more emerged wet-saline surface area and more soil erosion during an arid phase occurred at ~2100 cal yr BP, interrupting the overall humid phase (Fig. 7). This phase could be correlated to a synchronous arid event described in Zoñar Lake between 2120 and 2050 cal yr BP (Martín-Puertas et al., 2008; Gázquez et al., 2023), and at Siles Lake at around 1900 yr BP (Carrión, 2007), which point to a regional arid event interrupting the overall humid IRHP. Indeed, quantitative moisture estimates based on gypsum stable isotopes from Zoñar Lake and LGA indicate a decrease in atmospheric relative humidity by 10–15‰ at ~2100 cal yr BP with respect to the wettest phase of the IRHP at ~2400 cal yr BP, coinciding with a rainfall decrease by at least 20% (Gázquez et al., 2023, 2025). However, in the available reconstructions, this regional arid event appears to correspond to a negative NAO phase, which is generally associated with enhanced humidity (Fig. 6). This discrepancy might reflect regional variability in the precipitation signal or chronological mismatches due to the age-control limitations in the compared precipitation records.

The pollen record and climate estimates from LGA also suggest persistent warm conditions during the IRHP in this area (Fig. 9). Warming produced the displacement of the thermomediterranean bioclimatic belt to higher elevation, spreading around the LGA area during the warmer IRHP and the displacement of the meso-mediterranean *Quercus* towards higher elevations (Figs. 8 and 9). In this way, *Quercus* decreased and many Poaceae species, including *Macrochloa tenacissima*, and the thermophilic *Pistacia lentiscus,* which abound in the lower elevation thermomediterranean vegetation belt (Rivas-Martínez, 1997), most likely colonized the area during warmer climate. Our LGA record through the T/M pollen ratio and climate estimates shows warmest conditions between 2500 and 1800 yr BP (Fig. 9) and agrees with other temperature paleoclimate reconstructions from Iberia (Bernal-Wormull et al., 2023), southern Spain (Ramos-Román et al., 2018; Jiménez-Moreno et al., 2023b, 2025b) and the western Mediterranean Sea (Rodrigo-Gámiz et al., 2014; Margaritelli et al., 2020; Fig. 9). The peak in temperature shown by the pollen occurred at ~2100 cal yr BP. Perhaps the arid event previously described at that time was related to higher evaporation due to the highest temperatures. The high abundance of thecamoebians ~2100 cal yr BP in the LGA record (Fig. 4) could also confirm nutrient enrichment and higher productivity in the lake environment, previously noticed by high total organic carbon content in the record (Jiménez-Moreno et al., 2025a). The Laguna de Medina record, also in southern Spain, shows a sedimentary gap between 2600 and 1900 yr BP and a hiatus of preserved pollen likely related to strong lake-level lowering and oxidation of pollen grains (Schroeder et al., 2020), most-likely caused by high evaporation due to this warming. Peaks in Ericaceae at 2400–2300 and 2100 cal yr BP could be fire related, especially the highest peak at 2100 cal yr BP, which was previously related to enhanced aridity (Fig. 4). Warmest conditions during the IRHP triggered frequent fires in the region, which also were more abundant due to a higher fuel-load following enhanced humid conditions (Jiménez-Moreno et al., 2013). Additionally, at ~2100 cal yr BP (~150 BCE) took place the “romanization” of this area with the establishment of many roman colonies concentrated in southern Iberia and major change in settlements, administration and farming intensification in this region (Moreno Escobar, 2025), which could have also enhanced human-made fire activity in the study area.

The decrease in *Quercus* (generating a decline in arboreal pollen) due to this altitudinal vegetation movement caused by warming was previously observed in other pollen records from southern Spain but was interpreted due to human impact in Zoñar Lake (Martín-Puertas et al., 2008), Laguna de las Madres (Stevenson, 1985; Stevenson and Harrison, 1992) and in Los Tollos lake (Carrión et al., 2024). Although the LGA record indicates that climate was the most important factor triggering the changes in the vegetation and sedimentation in the LGA lake and regionally, the slight increases in Cerealia, *Rumex* and *Plantago* during the IRHP (Fig. 10), could also indicate more anthropogenic influence at that time with the cultivation of cereals and ruderalisation of the agricultural environment in the vicinity of the lake.

5.4. Post-Roman period between ~1400 cal yr BP and Present (550 CE – Present)

Proxies from the LGA sedimentary sequence show generally dry, cool conditions over the past 1500 years (Figs. 6, 7 and 9), aligning with other post-IRHP aridification trends observed in the western Mediterranean (Jiménez-Moreno et al., 2025a; Gázquez et al., 2025). However, this study also shows some slight variations in humidity and estimated temperature values in the past 1500 years detailed below.

5.4.1. Cold and dry conditions during the Early Middle Ages (EMA) between 1400 and 1100 cal yr BP (550 – 850 CE)

During the EMA (informally also known as Dark Ages or DA; ~1400 and 1100 cal yr BP; pollen subzone 3.1), the LGA sequence records peak *Quercus* abundance and thus minima in both the T/M pollen ratio and

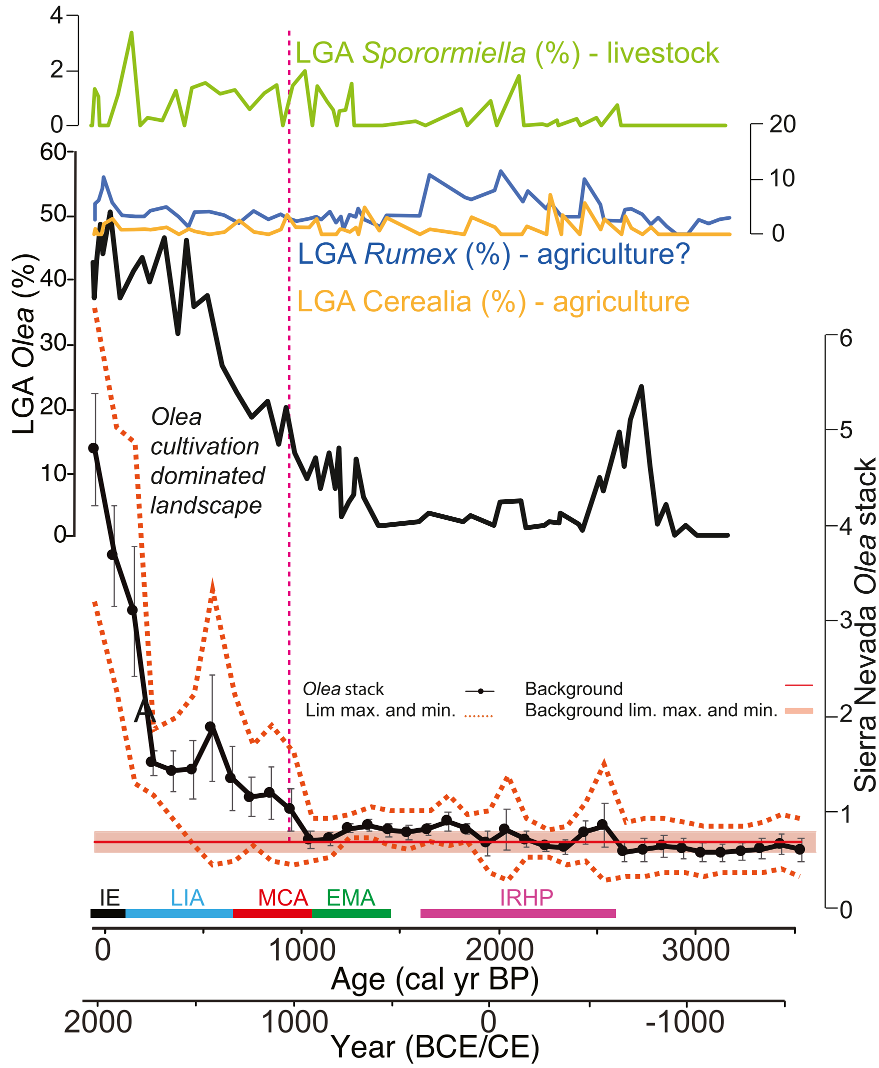

Fig. 10. Comparison of pollen proxies representing anthropogenic activity in the LGA and Sierra Nevada area, southern Spain, for the past ~3150 years. From bottom to top, synthetic *Olea* stack with error from the Sierra Nevada sites (Ramos-Román et al., 2019), and *Olea,* Cerealia and *Rumex* abundances (%) from LGA. The dashed red line indicates when the anthropogenic activity is clear in the study area. The duration of historic periods such as the Iberian Roman Humid Period (IRHP), Late Antique Little Ice Age (LALIA), Early Middle Ages (EMA), Medieval Climate Anomaly (MCA), Little Ice Age (LIA) and Industrial Era (IE) is indicated.

temperature estimates (averaging ~12 °C) (Fig. 9). The highest *Quercus* values coincide with a severe cooling event (~11.2 °C) at ~1250 cal yr BP, probably related, within dating uncertainties, to the Late Antique Little Ice Age (LALIA; between 1410 and 1290 cal yr BP or 540–660 CE; Büntgen et al., 2016) (Fig. 9). The progressive increasing trend in throughout the LGA sequence, peaking during the LALIA could have been due to the progressive cooling and decrease in seasonal contrast that occurred in the Middle and Late Holocene due to the decrease and increase in summer and winter insolation, respectively (Fig. 8). The LALIA cold event was most likely related to an intensification of the regional cooling trend by volcanic aerosol forcing, triggering a further cooling (Büntgen et al., 2016). Coldest conditions of the EMA are reached at at LGA at ~1100 cal yr BP, with a second cold event (Fig. 9).

Speleothem isotopic records from northern Spain also show cold conditions during the EMA, with especially cold intervals matching the timeframes of the LALIA and the ~1100 cal yr BP cold events (Bernal-Wormull et al., 2023; Bartolomé et al., 2024; Fig. 9). This suggests that different regions in Iberia were synchronically affected by this climatic variability at centennial-scales and recognized by local heterogenous signals.

Dry climate conditions are also interpreted for LGA during this period, deduced by minima in *Botrycoccus* and the sediment geochemistry (Fig. 6; Jiménez-Moreno et al., 2025a). Aridity triggered enhanced erosion, evidenced by a peak of MS and *Glomus* between 1400 and 1300 cal yr BP, and lowered lake levels, generating an increase in marginal lake surface area and aquatic macrophytes (Fig. 7). Coeval charcoal and Ericaceae peaks at ~1300 cal yr BP could indicate enhanced fire activity due to arid climatic conditions around LGA (Fig. 7).

Arid conditions prevailing during the EMA are also reflected in other pollen records across the region, which show declines in forest taxa and reconstructed precipitation (Ilvonen et al., 2022; Fig. 6). This reduction in forest cover is particularly evident in areas such as Doñana (Jiménez-Moreno et al., 2015), the Guadiana Valley in Portugal (Fletcher et al., 2007), and the Padul and Sierra Nevada regions (Ramos-Román et al., 2018; Mesa-Fernández et al., 2018; Jiménez-Moreno et al., 2013, 2022). Comparable trends in vegetation are also recorded in the Alboran Sea, in cores MD95–2043 and ODP 976 (Combourieu Nebout et al., 2009; Fletcher et al., 2013). Also using pollen records from the region, Camuera et al. (2023) identified significant drought phases with particularly severe events occurring at 1255–1225 cal yr BP (695–725 CE) and 1195–1180 cal yr BP (755–770 CE) (Fig. 6). Other evidences of enhanced aridity beginning at 1400 cal yr BP come from pronounced desiccation documented at

Laguna de Medina (Reed et al., 2001) and decreases in Mg/Al and Rb/Al ratios in the Alboran Sea and Lake Zoñar indicating reduced precipitation (Martín-Puertas et al., 2010; Fig. 6). In addition, gypsum speleothem growth in the southeastern Iberian Peninsula ceased at approximately 1200 cal yr BP, likely due to reduced cave water infiltration (Gázquez et al., 2020). Concurrently, lake levels declined markedly across southwestern and central Europe (Magny, 2004; Martín-Puertas et al., 2010). Paleoclimate reconstructions further suggest that a persistently positive phase of the NAO likely dominated the EMA after 1300 cal yr BP and recording a peak around 1250 cal yr BP (Olsen et al., 2012; Baker et al., 2015; Fig. 6), contributing to reduced winter precipitation and generally arid conditions across the region.

Cold and arid conditions, at least episodically, contributed to major plague outbreaks, large-scale human migrations, significant political instability, reduced urban life, and cultural transition during the EMA in Iberia: the collapse of the Western Roman Empire, the Visigothic kingdom's establishment and subsequent Muslim conquest in 711 CE (1239 cal yr BP) (Büntgen et al., 2016; Camuera et al., 2023).

5.4.2. The warmer and arid Medieval Climate Anomaly (MCA) between ~1100 and 600 cal yr BP (~850 and 1350 CE)

The MCA (900–1300 CE; Moreno et al., 2012) at LGA is characterized by an increasing trend in the T/M pollen ratio and in temperature estimates between ~1100 and 600 cal yr BP (pollen subzone 3.2), with two maxima in temperature at ~900 and 700 cal yr BP (~1050 and 1250 CE; Fig. 9) reaching peak values of ~14 ºC. These results align with the previously published chironomid-based and long-chain diol index (LDI)-derived temperature records from Sierra Nevada (García-Alix et al., 2020; Jiménez-Moreno et al., 2023b; 2025b; Fig. 9) and other studies suggesting that the Iberian Peninsula and the western Mediterranean experienced relatively warm conditions during the MCA (Moreno et al., 2012; Margaritelli et al., 2020).

Dry conditions also characterized most of the MCA (Fig. 6). This agrees with Camuera et al. (2023), who identified significant drought phases particularly severe events occurring at ~1050–1015 cal yr BP (~900–935 CE), and ~875–810 cal yr BP (~1075–1140 CE; Fig. 6). However, an increase in humidity is observed during the last part of the MCA, between ~750 and 600 cal yr BP (~1200 – 1350 CE), indicated by a peak in *Botryococcus* (Fig. 6).

High fire activity is registered in LGA during the MCA, with the highest charcoal concentrations at ~1100 cal yr BP (~850 CE) and ~850 cal yr BP (~1100 CE). A peak of the fire-related Ericaceae is also noticed at ~1000 cal yr BP (Fig. 4), which could further indicate enhanced fire activity at the LGA area at this time. Warm and dry overall climatic conditions at this time could have triggered enhanced fire activity in the study area but it could have also been related to anthropogenic activity, as it coincides with the long period of conflict that affected the studied region during the long revolt of Umar ibn Hafsun against the Emirate of Cordoba from 880 to 918 CE. During this period, the nearby town of Archidona changed sides several times, suffering sieges and raids. At the end of the conflict, Archidona went from being the capital of the Malaga province to being practically uninhabited, with the capital status passing to the city of Málaga (Martínez Enamorado, 2009).

Persistent positive NAO conditions dominated the MCA (Moreno et al., 2012; Olsen et al., 2012; Baker et al., 2015; Fig. 6), contributing to reduced winter precipitation and generally arid conditions across the region.

5.4.3. Little Ice Age (LIA) from 600 to 100 cal yr BP (1350–1850 CE) and Industrial Era (IE) (100 cal yr BP (1850 CE) - Present) (Pollen zone 4)

After the warm MCA, the T/M pollen ratio indicates colder conditions during the LIA with two minima in pollen-estimated temperatures of ~11.5 and 12 ºC at ~300 and 200 cal yr BP (Fig. 9). Overall dry conditions characterize the LGA record during the beginning of the LIA (Fig. 6). However, a return to more humid conditions occurred again between ~300 and 200 cal yr BP suggested by the peak in *Botryococcus* and geochemical composition as shown by the XRF PC1 (Jiménez-Moreno et al., 2025a; Fig. 6). NAO reconstructions show more negative phases during the LIA that could have triggered more precipitation in the area (Olsen et al., 2012; Baker et al., 2015; Fig. 6). The LIA ended with enhanced arid conditions at LGA centered at ~150 cal yr BP, te return to more positive NAO phases (Olsen et al., 2012; Baker et al., 2015) and the transition from colder to warmer temperature conditions between 150 and 100 cal yr BP (Fig. 6).

The IE is characterized at LGA by more humid (peak in *Botryococcus* between 37 and −6 cal yr BP) and generally warmer conditions than during the LIA (Fig. 9). More humid conditions during the IE would also agree with the pollen precipitation estimates from the southern Iberian Peninsula (Ilvonen et al., 2022; Camuera et al., 2023) and the Mg/Al elemental ratio from ODP 976 in the Alboran Sea (Martín-Puertas et al., 2010). However, this last maximum of *Botryococcus* at 0 cal yr BP could also be the result of enhanced lake productivity due to human-induced eutrophication likely due to the use of fertilizers in the nearby crops since ~1944 CE (Jiménez-Moreno et al., 2025a), rather than purely climatic forcing.

Pollen-based temperature estimations in the last decades oscillated considerably, from a minimum around 12 ºC at 1998 CE to a maximum of 14.1 ºC at 2003 CE (Fig. 9). This rapid temperature change could be related to recent global warming, such as the one observed in other temperature estimations from southern Iberia (García-Alix et al., 2020; Jiménez-Moreno et al., 2023b; 2025b; Fig. 9), or to the bias introduced by agriculture and land modification by humans on the vegetation and thus the pollen sedimentation (see chapter below). The most recent estimated temperature agrees within error ranges with instrumental data from the area of 14.8 ºC (WorldClim v2.1; Fick and Hijmans, 2017)

The charcoal concentration decreased in the past centuries until present (Fig. 7). This could have been due to fire suppression by humans caused by the strong modification of the landscape around LGA in the past millennium (see also chapter below).

5.4.4. Anthropogenic impact in the past millennium: from Mediterranean landscape to intensive Olea (olive) cultivation

Olive (*Olea europaea* L.) is the Mediterranean's dominant tree crop and a vital economic driver, especially in Spain (Ramos-Román et al., 2019). Pollen records trace olive cultivation since ~2500 cal yr BP, with widespread Roman expansion (~2000 cal yr BP), across Iberia and North Africa (Kehoe, 1988; Martín-Puertas et al., 2008; Langgut et al., 2019).

In these records, human activity is identified when the *Olea* pollen percentages experience a sudden increase, not accompanied by a rise in other Mediterranean sclerophyllous trees, and corroborated by consistent archaeological evidence (Langgut et al., 2019). In this respect, the LGA *Olea* pollen data show an increase between ~2800 and 2500 cal yr BP (Fig. 10). This agrees with the long-term trends in olive abundance from the nearby Sierra Nevada area for the last ~4500 cal yr BP, developed using a Z-score–based synthetic reconstruction of *Olea* pollen occurrences of seven independent time series, which shows a slight increasing trend beginning at ~2700 cal yr BP during the IRHP (Ramos-Román et al., 2019; Fig. 10). The Lake Zóñar pollen records, from Córdoba (inland Andalusia), also shows continuous *Olea* occurrences since 2700 cal yr BP (Valero Garcés et al., 2006; Martín-Puertas et al., 2008). This *Olea* increase, accompanied by *Quercus*, could have been due to the expansion of this species in the area due to warmer and more humid conditions associated with persistent negative NAO conditions (Martín-Puertas et al., 2009; see more discussion above). However, this *Olea* increase is coetaneous with the establishment of a series of Phoenician colonies along the South Iberian coast (Caro et al., 2025). It is well known that Phoenician colonization in this period had important consequences in western Mediterranean agriculture and the exploitation of vegetation in colonized areas (Rodríguez-Ariza et al., 2021). Distinguishing between climate-driven natural expansions of

Olea and increases related to early olive arboriculture remains challenging (Di Rita and Magri, 2009; Mercuri et al., 2013). Consequently, it is unclear whether this early *Olea* increase in southern Spain reflects olive cultivation or a natural response of Mediterranean vegetation to favorable climatic conditions.

A marked expansion of olive cultivation in LGA and Sierra Nevada occurred at ~1000 cal yr BP (950 CE), with *Olea* pollen showing a rapid increase that continues, with some variability, until present (Fig. 8). This expansion coincides with the establishment of predominantly positive NAO conditions and the onset of the MCA (Moreno et al., 2012), a generally warm and arid period that would not have favored the natural expansion of olive trees (see discussion above). The mismatch between climatic conditions and *Olea* pollen increase suggests a strong anthropogenic signal. Also, the exponential-like increase strongly suggests a dominant anthropogenic forcing rather than a purely climate-driven expansion. Similar increases in olive pollen during the last millennium have been reported in other sites from southern (Carrión et al., 2007) and northern Spain (Pérez-Sanz et al., 2013) and are associated with intensified agricultural activity. This phase partially overlaps with the agricultural intensification during the Muslim period after the cited revolt of Umar ibn Hafsun (950–550 cal yr BP; 1000–1450 CE), characterized by the expansion and intensification of irrigated crops, including olives in different regions (Ramos-Román et al., 2018). In this context, a rapid increase in *Olea* pollen not accompanied by a rise in other Mediterranean forest taxa (see the opposite trends of *Quercus*), especially when supported by archaeological or archaeobotanical evidence, is considered a reliable indicator of human-driven olive cultivation (Langgut et al., 2019). Therefore, the expansion of *Olea* marks the regional establishment of modern and intense agropastoral activities in the LGA area.

Following slights reductions during the Little Ice Age (LIA), *Olea* pollen occurrences from LGA show its maxima since mid-XXth century (between 1913 and 1965 CE), coinciding with the Industrial Era and the beginning of intensive olive crop irrigation in the study area (Hidalgo Moya et al., 2007), which also produced a critical lake lowering and gypsum sedimentation (Jiménez-Moreno et al., 2025a; Fig. 6). Anthropogenic impact maxima are confirmed by the expansion of ruderals such as *Plantago* (maxima at 1956 CE), indicating intensive land use. The continuous occurrence of *Sporormiella* with peak values ~100 cal yr BP also confirms enhanced grazing by domesticated livestock in the LGA area during the IE (Fig. 10).

6. Conclusions

The high-resolution palynological record from LGA, covering the past ~3150 years, shows long-term vegetation trends driven by declines in summer insolation and seasonality. This solar forcing triggered a gradual decrease in *Pinus* and a concurrent increase in *Quercus*. These long-term trends were modulated by centennial-scale climate variability, shown by multiproxy data from the LGA record, including the thermomediterranean/mesomediterranean forest pollen ratio, *Botryococcus* algae abundance, and sedimentary and geochemical data. Ultimately, this study indicates that temperature variations controlled elevational migration of vegetation, while the regional lake level was primarily governed by precipitation and humidity oscillations (the precipitation/evaporation balance). In this way, the pre-Roman period (~3150–2600 cal yr BP) was characterized by predominantly arid conditions, featuring an initial warm phase followed by a distinct cooling trend after 3000 cal yr BP. This was succeeded by the IRHP (~2600–1400 cal yr BP), which stood as the warmest and most humid interval of the record, despite a brief, severe arid episode ~2100 cal yr BP. A sharp transition to cold and dry conditions characterized the EMA (~1400–1100 cal yr BP), including temperature minima at ~1250 cal yr BP, likely associated with the LALIA, and at ~1100 cal yr BP. The subsequent MCA (~1100–600 cal yr BP; ~850–1350 CE) brough a return to warmer temperatures under predominantly arid conditions, although a shift toward higher humidity occurred during its final stages (~750–600 cal yr BP; ~1200–1350 CE). Climate variability intensified during the LIA (~600–150 cal yr BP; 1350–1800 CE), characterized by severe cold phases at ~600–450 cal yr BP (1350–1500 CE) and at ~300–200 cal yr BP (1650–1750 CE), a brief warming phase (~420–380 cal yr BP; 1530–1570 CE) and a final transition toward acute aridity ~150 cal yr BP (~1800 CE). Finally, the IE is characterized by generally warmer and more humid conditions relative to the preceding LIA baseline.

Beyond reconstructing regional Late Holocene climate variability, the LGA record highlights the coupled sensitivity and resilience of Mediterranean lacustrine ecosystems to natural and anthropogenic forcing. Throughout most of the record, vegetation and lake-level dynamics closely tracked centennial-scale climate variability driven by persistent NAO phases, indicating a climate-dominated baseline system. However, during the last millennium, and most acutely since the IE, intensive land use and widespread *Olea* cultivation have increasingly modulated and amplified these ecological responses. Past warm and humid intervals, particularly the IRHP, offer historical analogues for future Mediterranean scenarios where warming will interact with changing water availability and intensified land management. These findings underscore that future vulnerability of Mediterranean wetlands will depend not only on climatic change, but also on the intensity of human landscape transformation.

CRediT authorship contribution statement

Lu Chenao: Software, Methodology. **Francisco J. Jiménez-Espejo:** Writing – review & editing. **Erik J. de Boer:** Writing – review & editing, Investigation, Formal analysis. **José S. Carrión:** Writing – review & editing. **Jimenez-Moreno Gonzalo:** Writing – review & editing, Writing – original draft, Visualization, Methodology, Investigation, Funding acquisition, Formal analysis, Conceptualization. **Antonio García-Alix:** Writing – review & editing, Investigation, Funding acquisition, Conceptualization. **Jon Camuera:** Writing – review & editing, Methodology, Formal analysis. **Fernando Gázquez:** Writing – review & editing, Investigation. **Lucía Martegani:** Writing – review & editing. **Aurora Castillo-Baquera:** Writing – review & editing. **Marta Rodrigo-Gámiz:** Writing – review & editing. **Miguel Rodríguez-Rodríguez:** Writing – review & editing.

Declaration of Competing Interest

The authors declare that they have no known competing financial interests or personal relationships that could have appeared to influence the work reported in this paper.

Acknowledgements

This study was supported by projects PID2021-125619OB-C21/C22, PID2021-123980OA-I00 (GYPCLIMATE), RED24-153734-T (PALEONET) and CNS2025-165139 (CLIMGYP), funded by the Ministerio de Ciencia e Innovación of Spain, the Agencia Estatal de Investigación and the Fondo Europeo de Desarrollo Regional FEDER MCIN/AEI/10.13039/501100011033/FEDER, UE" and CGL2017-85415-R,; Junta de Andalucía I+D+i Junta de Andalucía 2020 Retos P-20-00059, UGR-FEDER B-RNM-144-UGR18, UGR-FEDER A-RNM-336-UGR20, Project cofinanced by FEDER and LifeWatch-Eric LifeWatch-2019-10-UGR-01 and the research group RNM-190 (Junta de Andalucía). F.G acknowledges the Ramón y Cajal fellowship, RYC2020-029811-I de la Agencia Estatal de Investigación and the grant PPIT-UAL, Junta de Andalucía-FEDER 2022-2026 (RyC-PPI2021-01). L.M. was funded by the FPU21/06924 grant of the Ministerio de Educación y Formación Profesional of Spain. J.C. acknowledges funding from the Junta de Andalucía through the postdoctoral contract DGP_POST_2024_00267. M.R.G. acknowledges funds from project C-EXP-201-UGR23 funded by the Consejería de

Universidad, Investigación e Innovación and the European Union by the Program FEDER Andalucía 2021-2027. J.S.C. acknowledges projects HOMEDSCAPE (PID2022-136832NB-100) and Fundación Séneca (22525/PI/24). We thank Raef Minwer-Barakat Requena and Alejandro López-Avilés who helped with the sediment sampling and the XRF scanning. We are grateful to the keepers of the Natural Reserve of Lagunas de Archidona, and specially to África Lupión for support during field surveys and for providing historical monitoring data of the lake. Funding for open access charge: Universidad de Granada / CBUA. This paper benefited from the comments and suggestions of two anonymous reviewers and the Editor in Chief Prof. Zicheng Yu.

Data availability

https://drive.google.com/drive/folders/1paXMiu-v9O8swK2QZn6JZDb-zU8Fjv4kj?usp=drive_link

Pollen data Laguna Grande de Archidona (Google Drive)

References

Alba-Sánchez, F., Abel-Schaad, D., López-Sáez, J.A., Sabariego-Ruiz, S., Sebastián Pérez-Díaz, S., Luelmo-Lautenschlaeger, R., Garrido-García, J.A., 2021. Early anthropogenic change in western Mediterranean mountains (Sierra Nevada, SE Spain). Anthropocene 33, 100278.

Anderson, R.S., Homola, R.L., Davis, R.B., Jacobson Jr., G.L., 1984. Fossil remains of the mycorrhizal fungal Glomus fasciculatum complex in postglacial lake sediments from Maine. Can. J. Bot. 62, 2325–2328.

Anderson, R.S., Jiménez-Moreno, G., Carrión, J.S., Pérez-Martínez, C., 2011. Holocene vegetation history from Laguna de Río Seco, Sierra Nevada, southern Spain. Quat. Sci. Rev. 30, 1615–1629.

Büntgen, U., Myglan, V., Ljungqvist, F., et al., 2016. Cooling and societal change during the Late Antique Little Ice Age from 536 to around 660 AD. Nat. Geosci. 9, 231–236.

Baker, A., Hellstrom, J.C., Kelly, B.F.J., Mariethoz, G., Trouet, V., 2015. A composite annual-resolution stalagmite record of North Atlantic climate over the last three millennia. Sci. Rep. 5, 10307.

Baker, A.G., Bhagwat, S.A., Willis, K.J., 2013. Do dung fungal spores make a good proxy for past distribution of large herbivores? Quat. Sci. Rev. 62, 21–31.

Bartolomé, M., Moreno, A., Sancho, C., Cacho, I., Stoll, H., Haghipour, N., Belmonte, Á., Spötl, C., Hellstrom, J., Edwards, R.L., Cheng, H., 2024. Reconstructing hydroclimate changes over the past 2500 years using speleothems from Pyrenean caves (NE Spain). Clim 20, 467–494.

Bernal-Wormull, J.L., Moreno, A., Bartolomé, M., Arriolabengoa, M., Pérez-Mejías, C., Iriarte, E., Osácar, C., Spötl, C., Stoll, H., Cacho, I., Edwards, R.L., Cheng, H., 2023. New insights into the climate of northern Iberia during the Younger Dryas and Holocene: The Mendukilo multi-speleothem record. Quat. Sci. Rev. 305, 108006.

Beug, H.J., 1961. Leitfaden der Pollenbestimmung, 1. Fischer, Stuttgart, p. 63.

Boudreau, E.A., Galloway, J.M., Patterson, R.T., Kumar, A., Michel, F.A., 2005. A paleolimnological record of Holocene climate and environmental change in the Temagami region, northeastern Ontario. J. Paleolimnol. 33, 445–461.

Camuera, J., Jiménez-Moreno, G., Ramos-Román, M.J., García-Alix, A., Toney, J.L., Anderson, R.S., Jiménez-Espejo, F.J., Kaufman, D., Bright, J., Webster, C., Yanes, Y., Carrión, J.S., Ohkouchi, N., Suga, H., Yamame, M., Yokoyama, Y., Martínez-Ruiz, F., 2018. Orbital-scale environmental and climatic changes recorded in a new ~ 200,000-year-long multiproxy sedimentary record from Padul, southern Iberian Peninsula. Quat. Sci. Rev. 198, 91–114.

Camuera, J., Jiménez-Moreno, G., Ramos-Román, M.J., García-Alix, A., Toney, J.L., Anderson, R.S., Jiménez-Espejo, F., Bright, J., Webster, C., Yanes, Y., Carrión, J.S., 2019. Vegetation and climate changes during the last two glacial-interglacial cycles in the western Mediterranean: A new long pollen record from Padul (southern Iberian Peninsula). Quat. Sci. Rev. 205, 86–105.

Camuera, J., Jiménez-Espejo, F.J., Soto-Chica, J., Jiménez-Moreno, G., García-Alix, A., Ramos-Román, M.J., Ruha, L., Castro-Prieto, M., 2023. Drought as a possible contributor to the Visigothic Kingdom crisis and Islamic expansion in the Iberian Peninsula. Nat. Commun. 14, 5733.

Caro, J.L., Suárez Padilla, J., Mora Serrano, B., 2025. Cronología y temporalidad de los inicios de la Edad de Hierro en la Bahía de Málaga: la primera presencia fenicia y su impacto en las poblaciones locales. Spal 2 (34), 31–69.

Carrara, P.E., Mode, W.N., Rubin, M., 1984. Deglaciation and postglacial timberline in the San Juan Mountains, Colorado. Quat. Res. 21, 42–55.

Carrión, J.S., Sánchez-Gómez, P., Mota, J.F., Yll, E.I., Chaín, C., 2003. Fire and grazing are contingent on the Holocene vegetation dynamics of Sierra de Gádor, southern Spain. Holocene 13, 839–849.

Carrión, J.S., Fuentes, N., González-Sampériz, P., Quirante, L.S., Finlayson, J.C., Fernández, S., Andrade, A., 2007. Holocene environmental change in a montane region of southern Europe with a long history of human settlement. Quat. Sci. Rev. 26, 1455–1475.

Carrión, J.S., Fernández, S., González-Sampériz, P., Gil-Romera, G., Badal, E., Carrión-Marco, Y., López-Merino, L., López-Sáez, J.A., Fierro, E., Burjachs, F., 2010. Expected trends and surprises in the Lateglacial and Holocene vegetation history of the Iberian Peninsula and Balearic Islands. Rev. Palaeobot. Palynol. 162, 458–476.

Carrión, J.S., Ochando, J., Michelangeli, F., Jiménez-Espejo, F., Ojeda, F., Amorós, G., Munuera, M., Marín-Arroyo, A.B., Penélope, González-Sampériz, Rodríguez-Vidal, J., Di Rita, F., Magri, D., 2024. Tracing 40,000 years of vegetation change in the Baetic-Rifan biodiversity hotspot. Rev. Palaeobot. Palynol. 331, 105202.

Combourieu Nebout, N., Peyron, O., Dormoy, I., Desprat, S., Beaudouin, C., Kotthoff, U., Marret, F., 2009. Rapid climatic variability in the west Mediterranean during the last 25000 years from high resolution pollen data. Climate 5, 503–521.

Davis, B.A.S., Chevalier, M., Sommer, P., Carter, V.A., Finsinger, W., Mauri, A., Phelps, L. N., Zanon, M., Abegglen, R., Åkesson, C.M., Alba-Sánchez, F., Anderson, R.S., Antipina, T.G., Atanassova, J.R., Beer, R., Belyanina, N.I., Blyakharchuk, T.A., Borisova, O.K., Bozilova, E., Bukreeva, G., Bunting, M.J., Clò, E., Colombaroli, D., Combourieu-Nebout, N., Desprat, S., Di Rita, F., Djamali, M., Edwards, K.J., Fall, P. L., Feurdean, A., Fletcher, W., Florenzano, A., Furlanetto, G., Gaceur, E., Galimov, A. T., Gałka, M., García-Moreiras, I., Giesecke, T., Grindean, R., Guido, M.A., Gvozdeva, I.G., Herzschuh, U., Hjelle, K.L., Ivanov, S., Jahns, S., Jankovska, V., Jiménez-Moreno, G., Karpińska-Kołaczek, M., Kitaba, I., Kołaczek, P., Lapteva, E.G., Latałowa, M., Lebreton, V., Leroy, S., Leydet, M., Lopatina, D.A., López-Sáez, J.A., Lotter, A.F., Magri, D., Marinova, E., Matthias, I., Mavridou, A., Mercuri, A.M., Mesa-Fernández, J.M., Mikishin, Y.A., Milecka, K., Montanari, C., Morales-Molino, C., Mrotzek, A., Muñoz Sobrino, C., Naidina, O.D., Nakagawa, T., Nielsen, A.B., Novenko, E.Y., Panajiotidis, S., Panova, N.K., Papadopoulou, M., Pardoe, H.S., Pędziszewska, A., Petrenko, T.I., Ramos-Román, M.J., Ravazzi, C., Rösch, M., Ryabogina, N., Sabariego Ruiz, S., Salonen, J.S., Sapelko, T.V., Schofield, J.E., Seppä, H., Shumilovskikh, L., Stivrins, N., Stojakowits, P., Svobodova Svitavska, H., Święta-Musznicka, J., Tantau, I., Tinner, W., Tobolski, K., Tonkov, S., Tsakiridou, M., Valsecchi, V., Zanina, O.G., Zimny, M., 2020. The Eurasian Modern Pollen Database (EMPD), version 2. Earth Syst. Sci. Data 12, 2423–2445.

Di Rita, F., Magri, D., 2009. Holocene drought, deforestation and evergreen vegetation development in the Central Mediterranean: a 5500 year record from Lago Alimini Piccolo, Apulia, Southeast Italy. Holocene 19, 295–306.

Djamali, M., Cilleros, K., 2020. Statistically significant minimum pollen count in Quaternary pollen analysis; the case of pollen-rich lake sediments. Rev. Palaeobot. Palynol. 275, 104156.

Escobar, J., Brenner, M., Whitmore, T.J., Kenney, W.F., Curtis, J.H., 2008. Ecology of testate amoebae (thecamoebians) in subtropical Florida lakes. J. Paleolimnol. 40, 715–731.

Faegri, K., Iversen, J., 1989. Textbook of Pollen Analysis. Wiley, New York.

Fick, S.E., Hijmans, R.J., 2017. WorldClim 2: new 1km spatial resolution climate surfaces for global land areas. Int. J. Climatol. 37 (12), 4302–4315.

Fletcher, W., Boski, T., Moura, D., 2007. Palynological evidence for environmental and climatic change in the lower Guadiana valley (Portugal) during the last 13,000 years. Holocene 17, 479–492.

Fletcher, W.J., Debret, M., Sanchez Goñi, M.F., 2013. Mid-Holocene emergence of a low-frequency millennial oscillation in western Mediterranean climate: Implications for past dynamics of the North Atlantic atmospheric westerlies. The Holocene 23 (2), 153–166.

Fuentes, N., Carrión, J.S., Fernández, S., Nocete, F., Lizcano Prestel, R., Pérez, C., 2007. Análisis polínico de los yacimientos arqueológicos Cerro del Alcázar de Baeza y Eras del Alcázar de Úbeda (Jaén). An. De. Biol. ía 29, 85–93.

Gázquez, F., Bauska, T.K., Comas-Bru, L., Ghaleb, B., Calaforra, J.-M., Hodell, D.A., 2020. The potential of gypsum speleothems for paleoclimatology: Application to the Iberian Roman Humid Period. Sci. Rep. 10, 14705.

Gázquez, F., Jiménez-Espejo, F.J., Rodríguez-Rodríguez, M., Martegani, L., Voigt, C., Ruíz-Lara, D., Moreno, A., Valero-Garcés, B., Morellón, M., Martín-Puertas, C., 2023. Roman water management impacted the hydrological functioning of wetlands during drought periods. Sci. Rep. 13, 18815.

Gázquez, F., Voigt, C., Castillo-Baquera, A., García-Alix, A., Jiménez-Moreno, G., Jíménez-Espejo, F., Martegani, L., Rodrigo-Gámiz, M., Jiménez-Bonilla, A., Rodríguez-Rodríguez, M., 2025. Quantifying atmospheric humidity in the western Mediterranean during the Iron Age and the Roman Era. Geophys. Res. Lett. 52, e2025GL120424.

García-Alix, A., Jiménez-Espejo, F.J., Lozano, J.A., Jiménez-Moreno, G., Martínez-Ruiz, F., García Sanjuán, L., Aranda Jiménez, G., García Alfonso, E., Ruiz-Puertas, G., Anderson, R.S., 2013. Anthropogenic impact and lead pollution throughout the Holocene in Southern Iberia. Sci. Total. Environ. 449, 451–460.

García-Alix, A., Toney, J.L., Jiménez-Moreno, G., Pérez-Martínez, C., Jiménez, L., Rodrigo-Gámiz, M., Anderson, R.S., Camuera, J., Jiménez-Espejo, F.J., Peña-Angulo, D., Ramos-Román, M.J., 2020. Algal lipids reveal unprecedent warming rates in alpine areas of SW Europe during the Industrial Period. Clim 16, 245–263.

Gil-Romera, G., Carrión, J.S., McClure, S.B., Schmich, S., Finlayson, C., 2009. Holocene vegetation dynamics in mediterranean iberia: Historical contingency and climate-human interactions. J. Anthropol. Res. 65 (2), 271–285.

Grimm, E.C., 1987. CONISS: a FORTRAN 77 program for stratigraphically constrained cluster analysis by the method of incremental sum of squares. Comput. Geosci. 13, 13–35.

Guy-Ohlson, D., 1992. *Botryococcus* as an aid of the interpretation of palaeoenvironment and depositional processes. Palaeogeogr. Palaeoclimatol. Palaeoecol. 71, 1–15.

Haas, J.N., 1996. *Neorhabdocoela* oocytes – _palaeoecological indicators found in pollen preparations from the Holocene freshwater lake sediments. Rev. Palaeobot. Palynol. 91, 371–382.

Hammer, O., Harper, D.A.T., Ryan, P., 2001. Past: paleontological statistics software package for education and data analysis. Palaeontol. Electron. 4 (1), 9.

Hidalgo Moya, J., Vega Macías, V., Hidalgo Moya, J.C., 2007. Riego del olivar en Andalucía. Agricultura 896, 376–382.

Hurrell, J.W., Kushnir, Y., Ottersen, G., Visbeck, M., 2013. An Overview of the North Atlantic Oscillation. The North Atlantic Oscillation: Climatic Significance and Environmental Impact. American Geophysical Union, pp. 1–35.

Ilvonen, L., López-Sáez, J.A., Holmström, L., Alba-Sánchez, F., Pérez-Díaz, S., Carrión, J. S., Ramos-Román, M.J., Camuera, J., Jiménez-Moreno, G., Ruha, L., Seppä, H., 2022. Spatial and temporal patterns of Holocene precipitation change in the Iberian Peninsula. Boreas 51, 776–792.

IPCC, 2022. In: Portner, H.-O., Roberts, D.C., Tignor, M., Poloczanska, E.S., Mintenbeck, K., Alegría, A., Craig, M., Langsdorf, S., Löschke, S., Möller, V., Okem, A., Rama, B. (Eds.), Climate Change 2022: Impacts, Adaptation, and Vulnerability. Contribution of Working Group II to the Sixth Assessment Report of the Intergovernmental Panel on Climate Change. Cambridge University Press. Cambridge University Press, Cambridge, UK and New York, NY, USA, p. 3056.

Jiménez-Moreno, G., Anderson, R.S., 2012. Holocene vegetation ad climate change recorded in alpine bog sediments from the Borreguiles de la Virgen, Sierra Nevada, southern Spain. Quat. Res. 77, 44–53.

Jiménez-Moreno, G., Abdul Aziz, H., Rodríguez-Tovar, F.J., Pardo-Igúzquiza, E., Suc, J.-P., 2007. Palynological evidence for astronomical forcing in Early Miocene lacustrine deposits from Rubielos de Mora Basin (NE Spain). Palaeogeogr. Palaeoclimatol. Palaeoecol. 252, 601–616.

Jiménez-Moreno, G., García-Alix, A., Hernández-Corbalán, M.D., Anderson, R.S., Delgado-Huertas, A., 2013. Vegetation, fire, climate and human disturbance history in the southwestern Mediterranean area during the late Holocene. Quat. Res. 79, 110–122.

Jiménez-Moreno, G., Rodríguez-Ramírez, A., Pérez-Asensio, J.N., Carrión, J.S., López-Sáez, J.A., Villarías-Robles, J.J., Celestino-Pérez, S., Cerrillo-Cuenca, E., León, A., 2015. Impact of late-Holocene aridification trend, climate variability and geodynamic control on the environment from a coastal area in SW Spain. Holocene 25, 607–617.

Jiménez-Moreno, G., García-Alix, A., Anderson, R.S., Ramos-Román, M.J., Camuera, J., Mesa-Fernández, J.M., Toney, J.L., Jiménez-Espejo, F.J., Carrión, J.S., López-Avilés, A., Rodrigo-Gámiz, M., Webster, C.E., 2022. Reconstruction of past environment and climate using wetland sediment records from the Sierra Nevada. In: Zamora, R., Oliva, M. (Eds.), The Landscape of the Sierra Nevada. Springer Nature Switzerland AG, pp. 95–114.

Jiménez-Moreno, G., Anderson, R.S., Markgraf, V., Staley, S.E., Fawcett, P.J., 2023a. Environmental and climate evolution in the Southwest USA since the last interglacial deduced from the pollen record from Stoneman lake, Arizona. Quat. Sci. Rev. 300, 107883.

Jiménez-Moreno, G., Heiri, O., García-Alix, A., Anderson, R.S., Jiménez-Espejo, F.J., López-Blanco, C., Jiménez, L., Pérez-Martínez, C., Rodrigo-Gámiz, M., López-Avilés, A., Camuera, J., 2023b. Holocene summer temperature reconstruction based on a chironomid record from Sierra Nevada, southern Spain. Quat. Sci. Rev. 319, 108343.

Jiménez-Moreno, G., Prat, N., Heiri, O., García-Alix, A., Anderson, R.S., Jiménez-Espejo, F.J., Camuera, J., López-Blanco, C., 2025b. Chironomid-based Holocene summer temperature dynamics from southern Spain. Quat. Sci. Rev. 369, 109647.

Jiménez-Moreno, G., García-Alix, A., Gázquez, F., Castillo-Baquera, A., Martegani, L., Rodríguez-Rodríguez, M., Rodrigo-Gámiz, M., Jiménez-Espejo, F.J., 2025a. Climate dynamics during the last 3000 years forced environmental and sedimentation changes in southern Spain: The Laguna Grande de Archidona record. Catena 256, 109123.

Juggins, S., 2022. C2 Version 1.8.0: Software for ecological and paleoecological data analysis and visualisation. University of Newcastle, Newcastle upon Tyne.

Keeley, J.E., Bond, W.J., Bradstock, R.A., Pausas, J.G., Rundel, P.W., 2012. Fire in Mediterranean Ecosystems: Ecology, Evolution and Management. Cambridge. Cambridge University Press.

Kehoe, D.P., 1988. The Economics of Agriculture on Roman Imperial Estates in North Africa. Vandenhoeck & Ruprecht.

López Fernández, M.L., López Fernández, M.S., 2018. Worldwide Bioclimatology Manual and Guide. Doc. Aljibe 5 (8), 1–157.

López-Avilés, A., Jiménez-Moreno, G., García-Alix, A., García-García, F., Camuera, J., Anderson, R.S., Sanjurjo-Sánchez, J., Chamorro, C.A., Carrión, J.S., 2022. Post-glacial evolution of alpine environments in the western Mediterranean region: the Laguna Seca record. Catena 211, 106033.

Langgut, D., Cheddadi, R., Carrión, J.S., Cavanagh, M., Colombaroli, D., Eastwood, W.J., Greenberg, R., Litt, T., Mercuri, A.M., Miebach, A., Roberts, N., Woldring, H., Woodbridge, J., 2019. The origin and spread of olive cultivation in the Mediterranean Basin: the fossil pollen evidence. Holocene, 0959683619826654.

Laskar, J., Robutel, P., Joutel, F., Gastineau, M., Correia, A.C.M., Levrard, B., 2004. A long-term numerical solution for the insolation quantities of the Earth. Astron. Astrophys. 428, 261–285.

Lionello, P., Malanotte-Rizzoli, P., Boscolo, R., Alpert, P., Artale, V., Li, L., Luterbacher, J., May, W., Trigo, R., Tsimplis, M., Ulbrich, U., Xoplaki, E., 2006. The Mediterranean climate: an overview of the main characteristics and issues. In: Lionello, P., Malanotte-Rizzoli, P., Boscolo, R. (Eds.), Mediterranean Climate Variability. Elsevier, Amsterdam, pp. 325–372.

Magny, M., 2004. Holocene climate variability as reflected by mid-European lake-level fluctuations and its probable impact on prehistoric human settlements. Quat. Int. 113, 65–79.

Margaritelli, G., Cacho, I., Català, A., barra, M., Bellucci, L.G., Lubritto, C., Rettori, R., Lirer, F., 2020. Persistent warm Mediterranean Surface Waters during the Roman period. Sci. Rep. 10, 10431.

Martínez Enamorado, V., 2009. Rayya y Archidona: una relación bien avenida a lo largo del Emirato de Córdoba Rayya. Rev. De. Invest. óN. Hist. órica De. la Comarc. Nororiental De. Málaga 5, 13–31.

Martín-Puertas, C., Valero-Garcés, B.L., Mata, M.P., González-Sampériz, P., Bao, R., Moreno, A., Stefanova, V., 2008. Arid and humid phases in southern Spain during the last 4000 years: the Zoñar Lake record, Córdoba. Holocene 18, 907–921.

Martín-Puertas, C., Valero-Garcés, B.L., Brauer, A., Mata, M.P., Delgado-Huertas, A., Dulski, P., 2009. The Iberian–Roman Humid Period (2600–1600 cal yr BP) in the Zoñar Lake varve record (Andalucía, southern Spain). Quat. Res. 71, 108–120.

Martín-Puertas, C., Jiménez-Espejo, F., Martínez-Ruiz, F., Nieto-Moreno, V., Rodrigo, M., Mata, M.P., Valero-Garcés, B.L., 2010. Late Holocene climate variability in the southwestern Mediterranean region: an integrated marine and terrestrial geochemical approach. Clim 6, 807–816.

MedECC, 2020. Climate and Environmental Change in the Mediterranean Basin - Current Situation and Risks for the Future. First Mediterranean Assessment Report. In: Cramer, W., Guiot, J., Marini, K. (Eds.), Union for the Mediterranean, Plan Bleu. UNEP/MAP, Marseille, France, p. 632.

Mederos Martin, A., 2021. The Chronology of the Late Bronze Age and the Early Iron Age in the Iberian Peninsula (1200-600 BC). In: E. Kaiser y W. Schier (Eds.): Time and Materiality: Periodization and Regional Chronologies at the Transition from Bronze to Iron Age in Eurasia (1200-600 BCE). Berlin, 109–236.

Mercuri, A.M., Bandini Mazzanti, M., Florenzano, A., Montecchi, M.C., Rattighieri, E., 2013. *Olea*, *Juglans* and *Castanea*: the OJC group as pollen evidence of the development of human-induced environments in the Italian peninsula. Quat. Int. 303, 24–42.

Mesa-Fernández, J.M., Jiménez-Moreno, G., Rodrigo-Gámiz, M., García-Alix, A., Jiménez-Espejo, F.J., Martínez-Ruiz, F., Anderson, R.S., Camuera, J., Ramos-Román, M.J., 2018. Vegetation and geochemical responses to Holocene rapid climate change in the Sierra Nevada (southeastern Iberia): the Laguna Hondera record. Climate 14, 1687–1706.

Moreno, A., Pérez, A., Frigola, J., Nieto-Moreno, V., Rodrigo-Gámiz, M., Martrat, B., González-Sampériz, P., Morellón, M., Martín-Puertas, C., Corella, J.P., Belmonte, A., Sancho, C., Cacho, I., Herrera, G., Canals, M., Grimalt, J.O., Jiménez-Espejo, F., Martínez-Ruiz, F., Vegas-Vilarrúbia, T., Valero-Garcés, B.L., 2012. The Medieval Climate Anomaly in the Iberian Peninsula reconstructed from marine and lake records. Quat. Sci. Rev. 43, 16–32.

Moreno Escobar, M.C., 2025. Patrones de asentamiento en la Bética Romana: un estudio sobre la romanización desde el análisis arqueológico espacial. E-book. BAR Publishing, Oxford, UK.

Olsen, J., Anderson, N.J., Knudsen, M.F., 2012. Variability of the North Atlantic Oscillation over the past 5,200 years. Nat. Geosci. 5, 808–812.

Pérez-Sanz, A., González-Sampériz, P., Moreno, A., Valero-Garcés, B., Gil-Romera, G., Rieradevall, M., Tarrats, P., Lasheras-Álvarez, L., Morellón, M., Belmonte, A., Sancho, C., Sevilla-Callejo, M., Navas, A., 2013. Holocene climate variability, vegetation dynamics and fire regime in the central Pyrenees: the Basa de la Mora sequence (NE Spain). Quat. Sci. Rev. 73, 149–169.

PAGES2k Consortium, 2017. A global multiproxy database for temperature reconstructions of the Common Era. Sci. Data 4, 170088.

Ramos-Román, M.J., Jiménez-Moreno, G., Anderson, R.S., García-Alix, A., Toney, J.L., Jiménez-Espejo, F.J., Carrión, J.S., 2016. Centennial-scale vegetation and North Atlantic oscillation changes during the late Holocene in the western mediterranean. Quat. Sci. Rev. 143, 84–95.

Ramos-Román, M.J., Jiménez-Moreno, G., Camuera, J., García-Alix, A., Anderson, R.S., Jiménez-Espejo, F.J., Carrión, J.S., 2018. Holocene climate aridification trend and human impact interrupted by millennial- and centennial-scale climate fluctuations from a new sedimentary record from Padul (Sierra Nevada, southern Iberian Peninsula). Climate 14, 117–137.

Ramos-Román, M.J., Jiménez-Moreno, G., Anderson, R.S., García-Alix, A., Camuera, J., Mesa-Fernández, J.M., Manzano, S., 2019. Climate controlled historic olive tree occurrences and olive oil production in southern Spain. Glob. Planet. Change 182, 102996.

Reed, J.M., Stevenson, A.C., Juggins, S., 2001. A multi-proxy record of Holocene climatic change in southwestern Spain: the Laguna de Medina, Cádiz. Holocene 11, 707–719.

Reimer, P.J., Austin, W.E.N., Bard, E., Bayliss, A., Blackwell, P.G., Bronk Ramsey, C., Butzin, M., Cheng, H., Edwards, R.L., Friedrich, M., Grootes, P.M., Guilderson, T.P., Hajdas, I., Heaton, T.J., Hogg, A.G., Hughen, K.A., Kromer, B., Manning, S.W., Muscheler, R., Palmer, J.G., Pearson, C., van der Plicht, J., Reimer, R.W., Richards, D.A., Scott, E.M., Southon, J.R., Turney, C.S.M., Wacker, L., Adolphi, F., Büntgen, U., Capano, M., Fahrni, S.M., Fogtmann-Schulz, A., Friedrich, R., Köhler, P., Kudsk, S., Miyake, F., Olsen, J., Reinig, F., Sakamoto, M., Sookdeo, A., Talamo, S., 2020. The IntCal20 Northern Hemisphere Radiocarbon Age Calibration Curve (0–55 cal kBP). Radiocarbon 62, 725–757.

Rivas-Martínez, S., 1987. Memoria del mapa de series de vegetación de España. Ministerio de Agricultura, Pesca y Alimentación, Madrid.

Rodríguez-Ariza, M.O., López Castro, J.L., Jerbania, I.B., Martín, A.M., Ferjaoui, A., Hahnmüller, V.M., Barrionuevo, C.A.P., Moreno, A.S., Khalfali, W., Jendoubi, K., 2021. Long-term human impact and forest management in the Phoenician and Roman city of Utica (Tunisia) (900 BC−500 AD). Holocene 31 (6), 943–953.

Rodrigo-Gámiz, M., Martínez-Ruiz, F., Rampen, S.W., Schouten, S., Sinninghe Damsté, J. S., 2014. Sea surface Temperature variations in the western Mediterranean Sea over the last 20 kyr: A dual-organic proxy (UK′37 and LDI) approach. Paleoceanography 29, 87–98.

Sanchez Goñi, M.S., Cacho, I., Turon, J.L., Guiot, J., Sierro, F., Peypouquet, J., et al., 2002. Synchroneity between marine and terrestrial responses to millennial scale climatic variability during the last glacial period in the Mediterranean region. Clim. Dynam 19 (1), 95–105.

Schroeder, T., López-Sáez, J.A., van't Hoff, J., Reichter, K., 2020. Unravelling the Holocene environmental history of south-western Iberia through a palynological study of Lake Medina sediments. The Holocene 30, 13–22.

Stevenson, A.C., 1985. Studies in the vegetational history of SW Spain. II. Palynological investigations at Laguna de las Madres, SW Spain. J. Biogeogr. 12, 293–314.
Stevenson, A.C., Harrison, R.J., 1992. Ancient forests in Spain: a model for land-use and dry forest management in south-west Spain from 4000 BC to 1900 AD. Proc. Prehist. Soc. 58, 227–247.
Telford, R.J., Birks, H.J.B., 2005. The secret assumption of transfer functions: problems with spatial autocorrelation in evaluating model performance. Quat. Sci. Rev. 24, 2173–2179.
Toney, J.L., Anderson, R.S., 2006. A postglacial paleoecological record from the San Juan Mountains of Colorado USA: fire, climate and vegetation history. Holocene 16, 505–517.
Valero-Garcés, B.L., González-Sampériz, P., Navas, A., et al., 2006. Human impact since medieval times and recent ecological restoration in a Mediterranean lake the Laguna Zoñar (Spain). J. Paleolimnol. 35 (3), 441–465.
Van Geel, B., Coope, G.R., van der Hammen, T., 1989. Palaeoecology and stratigraphy of the Lateglacial type section at Usselo (The Netherlands). Rev. Paleobot. Palynol. 60, 25–129.
Whitlock, C., Anderson, R.S., 2003. Fire history reconstructions based on sediment records from lakes and wetlands. In: Veblen, T.T., Baker, W.L., Montenegro, G., Swetnam, T.W. (Eds.), Fire and Climatic Change in Temperate Ecosystems of the Americas, 160. Springer-Verlag, New York, pp. 3–31.